

**SEMI-ANALYTICAL ESTIMATES OF PERMEABILITY
OBTAINED FROM CAPILLARY PRESSURE**

A Thesis

by

CAROLINE CECILE HUET

Submitted to the Office of Graduate Studies of
Texas A&M University
in partial fulfillment of the requirements for the degree of

MASTER OF SCIENCE

December 2005

Major Subject: Petroleum Engineering

**SEMI-ANALYTICAL ESTIMATES OF PERMEABILITY
OBTAINED FROM CAPILLARY PRESSURE**

A Thesis

by

CAROLINE CECILE HUET

Submitted to the Office of Graduate Studies of
Texas A&M University
in partial fulfillment of the requirements for the degree of

MASTER OF SCIENCE

Approved by:

Chair of Committee,
Committee Members,

Head of Department,

Thomas A. Blasingame
Maria A. Barrufet
Steven L. Dorobek
Stephen Holditch

December 2005

Major Subject: Petroleum Engineering

ABSTRACT

Semi-Analytical Estimates of Permeability

Obtained from Capillary Pressure. (December 2005)

Caroline Cécile Huet,

Dipl., Ecole Nationale Supérieure de Géologie de Nancy, France

Chair of Advisory Committee: Dr. Thomas A. Blasingame

The objective of this research is to develop and test a new concept for predicting permeability from routine rock properties. First, we develop a model predicting permeability as a function of capillary pressure. Our model, which is based on the work by Purcell, Burdine and Wyllie and Gardner models, is given by:

$$k = 10.66 \alpha \frac{\gamma^2}{2} (1 - S_{wi})^3 \phi^3 \int_0^1 \frac{1}{p_d^2} dS_w^*$$

Combining the previous equation and the Brooks and Corey model for capillary pressure, we obtain:

$$k = 10.66 \alpha \gamma^2 (1 - S_{wi})^3 \phi^3 \frac{1}{p_d^2} \left[\frac{\lambda}{\lambda + 2} \right]$$

The correlation given by this equation could yield permeability from capillary pressure (and vice-versa). This model also has potential extensions to relative permeability (*i.e.*, the Brooks and Corey relative permeability functions) — which should make correlations based on porosity, permeability, and irreducible saturation general tools for reservoir engineering problems where relative permeability data are not available.

Our study is validated with a large range/variety of core samples in order to provide a representative data sample over several orders of magnitude in permeability. Rock permeabilities in our data set range from 0.04 to 8700 md, while porosities range from 0.3 to 34 percent. Our correlation appears to be valid for both sandstone and carbonate lithologies.

ACKNOWLEDGEMENTS

I would like to sincerely thank the following:

Dr. Tom Blasingame, chair of my advisory committee, for his valuable guidance, intellectual contributions, and his patience in helping me bring this research to its completion.

Drs. Maria Barrufet and Steve Dorobek for serving as members of my advisory committee.

TABLE OF CONTENTS

		Page
CHAPTER I	INTRODUCTION.....	1
	1.1 Introduction.....	1
	1.2 Objectives.....	1
	1.3 Statement of the Problem.....	1
	1.4 Validation.....	3
	1.5 Summary and Conclusions.....	6
	1.6 Future Efforts.....	6
	1.7 Outline of This Thesis.....	6
CHAPTER II	LITERATURE REVIEW.....	8
	2.1 Definition, Measurements and Models of Capillary Pressure.....	8
	2.2 Definition of Permeability and Models.....	14
CHAPTER III	DEVELOPMENT OF A SEMI-ANALYTICAL ESTIMATE OF PERMEABILITY OBTAINED FROM CAPILLARY PRESSURE.....	30
	3.1 Development and Validation of New Model.....	30
	3.2 Results and Discussion.....	33
CHAPTER IV	SUMMARY, CONCLUSIONS, AND RECOMMENDATIONS FOR FUTURE WORK.....	43
	4.1 Summary.....	43
	4.2 Conclusions.....	44
	4.3 Recommendations for Future Work.....	45
	NOMENCLATURE.....	46
	REFERENCES.....	48
	APPENDICES.....	52
	VITA.....	54

LIST OF TABLES

TABLE		Page
2.1	Comparison of Different Techniques to Measure Capillary Pressure.	12
2.2	Van Baaren Empirical Data.....	19
2.3	Fractal Models.....	22
3.1	Summary Regression Statistics for k, p_d, λ — Power Law Models	36
3.2	Regression Summary for k	37
3.3	Regression Summary for p_d	38
3.4	Regression Summary for λ	40

LIST OF FIGURES

FIGURE	Page
1.1 Permeability correlation based on mercury capillary pressure data.	3
1.2 Displacement pressure (p_d) correlation — mercury p_c data	4
1.3 Pore geometric factor (λ) correlation — mercury p_c data	5
2.1 Force balance at a water-oil-solid interface	8
2.2 Fluid rise in a capillary tube.....	9
2.3 Full capillary pressure curve (1st drainage, 1st imbibition and 2nd drainage).....	10
2.4 Concept model for petrophysical systems as proposed by Archie	15
2.5 Logarithmic (permeability) correlation proposed by Archie.....	16
2.6 Jennings and Lucia (concept) plot of clean and shaly sands — clean sand model:.....	17
2.7 a) Cazier, <i>et al</i> data for South American reservoir systems.	
b) Berg power law model for permeability as a function of porosity and grain size..	17
3.1 Example correlation of Brooks-Corey $p_c(S_w)$ model to a typical core data set for this study a. Capillary pressure versus wetting phase saturation plot – Cartesian capillary pressure format.	
b. Capillary pressure versus wetting phase saturation plot – Logarithmic capillary pressure format	34
3.2 Capillary pressure versus normalized wetting phase saturation plot – Cartesian capillary pressure format.....	35
3.3 Dimensionless capillary pressure versus normalized wetting phase saturation plot – Log-Log format "Type curve" for capillary pressure.	35
3.4 Dimensionless capillary pressure versus dimensionless wetting phase saturation plot – Log-Log format "Type curve" for capillary pressure.....	36
3.5 Permeability correlation based on mercury capillary pressure data	38
3.6 Displacement pressure (p_d) correlation based on mercury capillary pressure data	39
3.7 Pore geometric factor (λ) correlation based on mercury capillary pressure data.	41

CHAPTER I

INTRODUCTION

1.1 Introduction

The principal objective of this work is to develop and document a "universal" model which provides a more consistent correlation of permeability with mercury capillary pressure data for a much wider range of rock types. We begin with a review of the models developed previously — and we then document the validation of our generalization of the Purcell¹-Burdine-Brooks-Corey $k(H_g)$ model.

1.2 Objectives

The overall objectives of this work are:

- To develop and validate a generalized relationship between permeability and capillary pressure;
- To develop specific correlations for permeability (k), capillary displacement pressure (p_d), and the pore geometry factor (λ) for the case of mercury (Hg) injection capillary pressure data;
- To attempt development of an "equation-of-state" for permeability.

1.3 Statement of the Problem

This study focuses on permeability and its prediction — the first part of the derivation follows the work of Wyllie and Gardner.³ Their model describes the porous media as a bundle of capillary tubes featuring a random connection of pore spaces. Some of the assumptions made are:

1. Two-phase immiscible displacement;
2. One dimensional linear flow;
3. Darcy's law is a valid model to describe the fluid flow.

The detailed derivation of the permeability-capillary pressure equations is given in Appendix A. The base relation of this derivation is: (similar to Wyllie and Gardner³)

$$k = 10.66 \frac{\beta \gamma^2}{n} (1 - S_{wi})^3 \phi^3 \int_0^1 \frac{1}{p_d^2} dS_w^* \dots\dots\dots (1.1)$$

Brooks and Corey⁴ presented the following model for capillary pressure:

$$p_c = p_d \left[\frac{S_w - S_{wi}}{1 - S_{wi}} \right]^{-\frac{1}{\lambda}} \dots\dots\dots (1.2)$$

This thesis follows the style and format of the *SPE Journal*.

where p_d is the "displacement pressure" and λ is the "pore geometric factor" and

$$S_w^* = \frac{S_w - S_{wi}}{1 - S_{wi}} \dots\dots\dots (1.3)$$

It is worth noting that Li⁵ has also provided a derivation of a capillary pressure model using fractals which has Eq. 5 as a limiting form. Substituting Eq. 1-2 into Eq. 1-1, we have:

$$k = 10.66 \frac{\beta}{n} \gamma^2 (1 - S_{wi})^3 \phi^3 \frac{1}{p_d^2} \left[\frac{\lambda}{\lambda + 2} \right] \dots\dots\dots (1.4)$$

According to Wyllie and Gardner,³ β and n are parameters that depend on the configurations of the porous network. Although Wyllie and Gardner do not provide any mechanism to determine the parameters, they do mention that n is equal to or greater than one for a natural porous media. " β is inserted to recognize the fact that flow through a tube of a radius r overemphasizes the impedance since it ignores the larger areas available for flow at either side if the constrictions formed where tubes abut." Wyllie and Gardner assumed that β is a constant for all pore sizes — however, they expected $\beta \geq 1$ and the magnitude of β to be a function of the average shape of pores in the medium.

Ali⁶ suggested the following models for computing β and n :

$$\beta = \frac{1}{\phi} \dots\dots\dots (1.5)$$

and

$$n = \frac{1}{(1 - S_{wi})} \dots\dots\dots (1.6)$$

Substituting Eqs. 1-6 and 1-5 into 1-4 gives:

$$k = 10.66 \alpha \gamma^2 (1 - S_{wi})^4 \phi^2 \frac{1}{p_d^2} \left[\frac{\lambda}{\lambda + 2} \right] \dots\dots\dots (1.7)$$

As an initial correlation model, we use

$$k = a_1 \frac{1}{(p_d)^{a_2}} \left[\frac{\lambda}{\lambda + 2} \right]^{a_3} (1 - S_{wi})^{a_4} \phi^{a_5} \dots\dots\dots (1.8)$$

1.4 Validation

To validate the model, we have used mercury injection capillary pressure data sets from the literature and industry sources (from the literature, we have selected cases from Purcell,¹ Archie,⁷ and Neasham⁸). Samples from sandstone and carbonate reservoirs are used — and we note that data obtained from synthetic rock samples were initially considered, but these were not used because we chose to only consider mercury injection capillary pressure data for this study. Approximately 120 data sets have been reviewed (with 89 data sets being used in our current work), with permeabilities ranging from 0.04 md to 8700 md and porosities ranging from 0.3 to 34 percent.

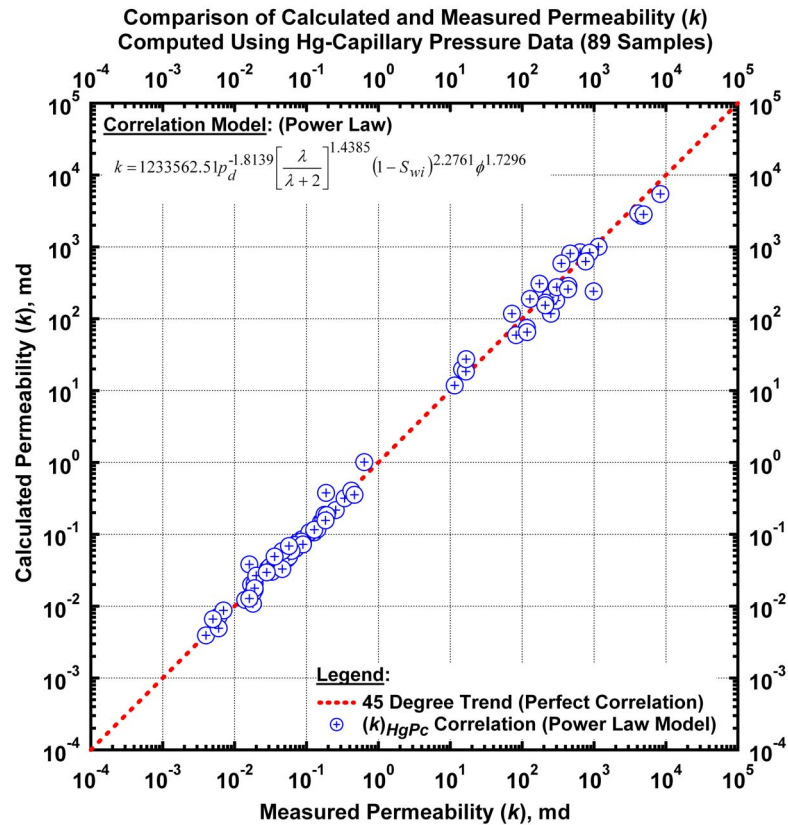


Figure 1.1 – Permeability correlation based on mercury capillary pressure data. Note an excellent correlation of calculated permeability data over 7 log-scales of variation in permeability.

Given core properties (k and ϕ), capillary pressure data (p_c - S_w profile), we applied the following steps:

- plot S_w versus p_c .
- determine p_{db} , S_{wb} and λ using the Brooks and Corey's model,
- use Eq. 7 to calculate the permeability (as consistency check), and
- calibrate/optimize the parameters in Eq. 1.8 using regression.

Fig. 1.1, which presents the results of this optimization, indicates excellent agreement between the measured permeabilities and those calculated from Eq. 1.8. We note that the same equation was used to calculate the entire permeability range — from low permeability (tight gas sands) to unconsolidated sands. From our work to date, the generalized relation (Eq. 1.8) appears to be universally valid for different lithologies. We will continue the validation process with additional data — and strive to access as much data as possible, including variable lithologies. We will note that, at this point in our research, we intend to focus uniquely on mercury (Hg) capillary pressure data sets — we will pursue all types of capillary pressure data (various fluid types *e.g.*, gas-water, gas-oil, and water oil and various measurement techniques, *e.g.*, centrifuge, porous plate, vapor desorption, *etc.*) for a general archive, but our primary focus (due to the availability and consistency of data) will be mercury capillary pressure data.

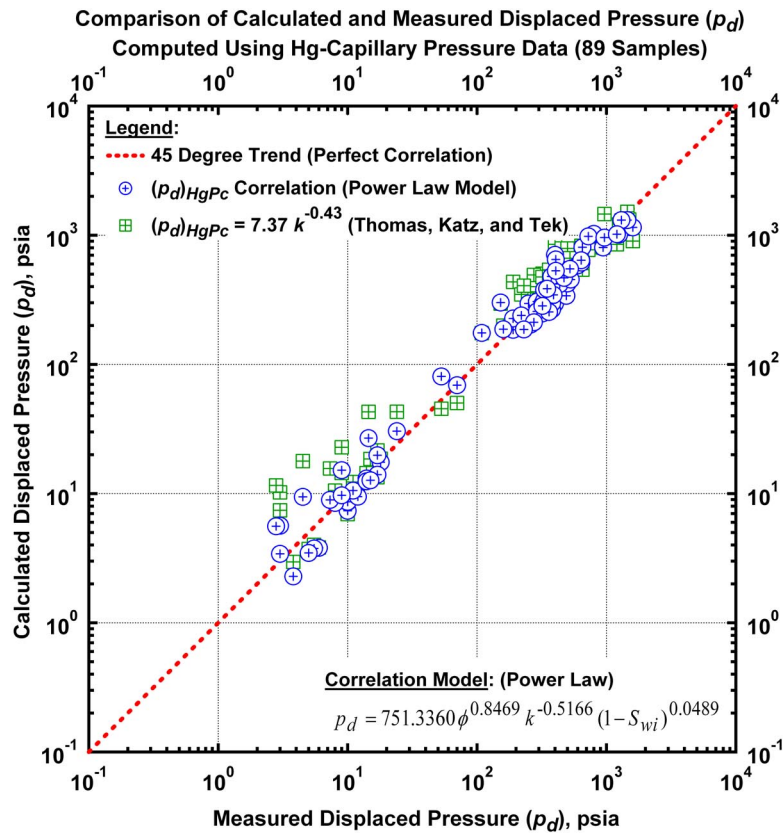


Figure 1.2 – Displacement pressure (p_d) correlation — mercury p_c data. Good correlation of data over 3 log-scales of displacement pressure.

We also correlate displacement pressure with permeability, porosity and irreducible saturation. **Fig. 1.2** presents the results of our initial (power law) correlation model which shows a good correlation of data over 3 log-scales of displacement pressure. The initial correlation model is given as:

$$p_d = b_1 \phi^{b_2} k^{b_3} (1 - S_{wi})^{b_4} \dots\dots\dots (1.9)$$

We correlate pore geometric factor (λ) with permeability, porosity, irreducible saturation and displacement pressure with the following model:

$$\lambda = c_1 \phi^{c_2} k^{c_3} (1 - S_{wi})^{c_4} p_d^{c_5} \dots\dots\dots (1.10)$$

Fig. 1.3 presents the results of this relation. The average error is about 18 percent.

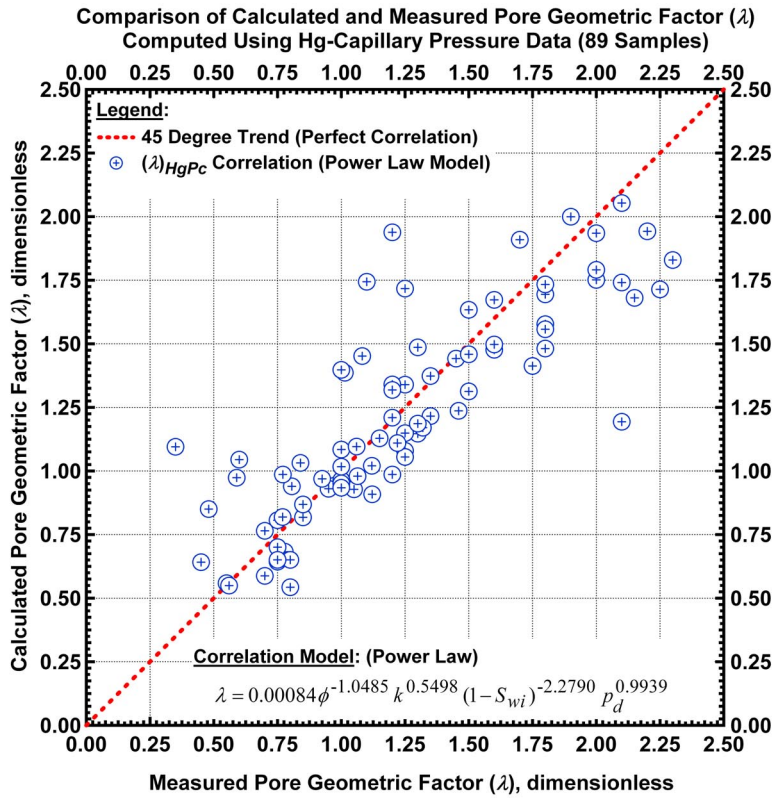


Figure 1.3 – Pore geometric factor (λ) correlation — mercury p_c data.

1.5 Summary and Conclusions

Permeability-Capillary Pressure Correlation

We have proposed, developed, and verified a new model to predict permeability from mercury capillary pressure data (Eq. 1.7). This equation is based on the relations of Purcell¹, Burdine², Brooks and Corey⁴ and Wyllie and Spangler.³ We also use the form of our new model to create a permeability correlation (Eq. 1.8) —which correlates permeability with: porosity (ϕ), irreducible wetting phase saturation (S_{wi}), displacement pressure (p_d), and the pore geometric factor (λ). We obtain very good agreement between the measured permeability values and those obtained from the optimized correlation.

This correlation is a work in progress — and as we continue to add data, we also expect to continue to observe the strong correlation of the input variables with permeability via our proposed models (see Appendix A). The results to date suggest that the correlating properties of the porous media (k , ϕ , S_{wi} , p_d , and λ) are not specifically dependent upon lithology — but rather, these properties uniquely quantify the fluid flow behavior of the porous medium. In that sense, we see this work as a generalized correlation for flow in porous materials — including soils, filters, sintered metals, bead packs, and porous rocks. We will continue to incorporate both sandstone and carbonate lithologies to validate the general model.

1.6 Future Efforts

Permeability Prediction from Capillary Pressure

We require more data samples to validate and extend the proposed relation. We also need to include more data from carbonate systems. At present, this correlation uses only mercury injection data. In the future we can also validate the correlation using p_c data obtained from other methods (*e.g.*, porous plate and centrifuge) — our initial efforts confirm such a validation, but we need to continue and extend this effort.

1.7 Outline of This Thesis

The outline of the proposed research thesis is as follows:

- Chapter I — Introduction
 - Research problem
 - Research objectives
 - Summary
- Chapter II — Literature Review
 - General concepts — capillary pressure, permeability
 - Capillary pressure models
 - Permeability correlations

- Chapter III — Development of a Semi-Analytical Estimate of Permeability Obtained from Capillary.
 - Statement of the problem
 - Capillary pressure model used for this development
 - Correlation of permeability.
 - Correlation of displacement pressure.
 - Correlation of pore geometry factor (λ).
- Chapter IV — Summary, Conclusions, and Recommendations for Future Work
 - Summary
 - Conclusions
 - Recommendations for future work
- Nomenclature
- References
- Appendices
 - Appendix A — Derivation of Permeability and Relative Permeability from Capillary Pressure
 - Appendix B — Derivation of a Function for the Normalization of Capillary Pressure Curves.
 - Appendix C — Comparison with Timur's Permeability Model
 - Appendix D — Summary of Data Used in this Study.
 - Appendix E — Correlations for Permeability (k) Derived from the Data in this Work.
 - Appendix F — Correlations for Displacement Pressure (p_d) Derived from the Data in this Work.
 - Appendix G — Correlations for Index of Pore Size Distribution (λ) Derived from the Data in this Work.
 - Appendix H — Non-Parametric Regressions Derived from the Data in this Work.
 - Appendix I — Library of Capillary Pressure versus Wetting Phase Saturation Plots – Cartesian Capillary Pressure Format.
 - Appendix J — Library of Capillary Pressure versus Wetting Phase Saturation Plots – Logarithmic Capillary Pressure Format.
 - Appendix K — Library of Capillary Pressure versus Normalized Wetting Phase Saturation Plots – Logarithmic Capillary Pressure Format.
 - Appendix L — Library of Dimensionless Capillary Pressure versus Normalized Wetting Phase Saturation Plots – Log-Log Format "Type Curve" for Capillary Pressure.
 - Appendix M — Library of Dimensionless Capillary Pressure versus Dimensionless Wetting Phase Saturation Plots – Log-Log Format "Type Curve" for Capillary Pressure.
 - Appendix N — Bibliography of Relevant Citations in Petrophysics.
- Vita

CHAPTER II

LITERATURE REVIEW

2.1 Definition, Measurements and Models of Capillary Pressure

Capillary Theory

Capillary pressure is defined as the pressure difference between the non-wetting and the wetting phases when two the miscible fluids come in contact with each other on a solid substrate. To understand the concept of wettability more clearly, we can look at the forces acting at a planar water-oil-solid interface as shown in **Fig. 2.1**.

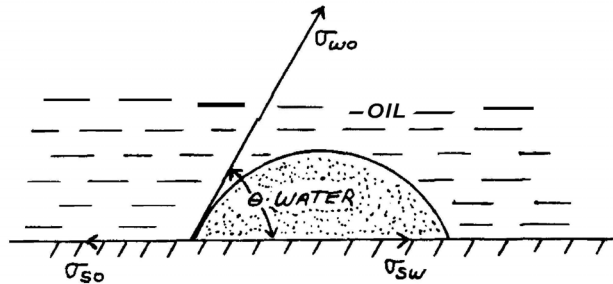


Figure 2.1 – Force balance at a water-oil-solid interface.

It is the balance of these forces that enables us to define wettability as an adhesion tension, which is written in terms of the surface forces:

$$A_T = \sigma_{so} - \sigma_{sw} \dots\dots\dots (2.1)$$

The term σ_{so} is the interfacial tension between the substrate and the oil and σ_{sw} is the interfacial tension between the substrate and the water. Interfacial tension can be thought of as the amount of force per unit length required to create a new surface between the two immiscible fluids. Since the forces must be in balance if there is no motion, the adhesion tension at the water/oil interface can also be written include the contact angle.

$$A_T = \sigma_{wo} \cos \theta \dots\dots\dots (2.2)$$

By convention the contact angle θ is measured through the denser phase. A positive A_T means that the denser phase preferentially wets the rock and a negative A_T indicates that the less dense fluid is the wetting phase. Now consider the rise of a fluid in a capillary tube as shown in **Fig 2.2**. Through a force balance, we can derive Eq. 2.3 for the capillary pressure, p_c , in that tube:

$$p_c = p_o - p_w = \frac{2\pi r A_T}{\pi r^2} \dots\dots\dots (2.3)$$

Where p_c is the pressure difference between the oil and the water at the oil-water interface and r the tube radius.

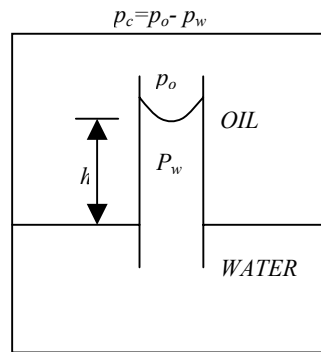


Figure 2.2 – Fluid rise in a capillary tube.

We can combine Eqs. 2.2 and 2.3 to define the capillary pressure in terms of the surface forces and the tube geometry:

$$p_c = \frac{2\sigma_{wo} \cos \theta}{r} \dots\dots\dots (2.4)$$

Equation (2.4) indicates the inverse relationship between pore throat size and capillary pressure. The equation also shows the absence of capillary pressure when the interfacial tension between fluid phases approaches zero. The classification of capillary pressure data based on geological facies is related to the variation of pore throat / pore body size distribution associated with each facies.

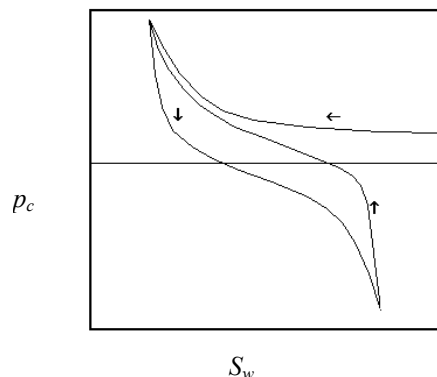


Figure 2.3 – Full capillary pressure curve (1st drainage, 1st imbibition and 2nd drainage).

Primary drainage capillary pressure curves are used to estimate the reservoir connate water saturation above the original oil-water or gas-water contact (**Fig. 2.3**). The irreducible water saturation can be determined from these data. The threshold pressure obtained from the primary drainage capillary pressure curve is used to determine the offset between the water-oil or gas-water contact and the free-water level. Drainage capillary pressure data can also be used to estimate the pore throat⁹ and pore body size distribution. Capillary pressure data can also be used to evaluate the integrity of the seal of the reservoir.

Methods of Capillary Pressure Measurements

There are three laboratory methods that are commonly used to measure primary drainage capillary pressure in a rock, (1) the porous plate (restored-state) method, (2) the centrifuge method, and (3) the mercury injection technique.

• **Porous Plate**

The porous plate technique¹⁰⁻¹³ employs a strongly water-wet semi-permeable membrane, typically made of porcelain, cellulose or fused glass, which has fine pores of uniform size. When saturated with a wetting phase, the plate exhibits a high threshold pressure to the entrance of a non-wetting phase. The core sample is exposed to the non-wetting phase and a differential pressure is applied between that phase and the external side of the plate. Thus, the non-wetting phase is forced into the core, as wetting phase is displaced into and through the porous plate. The process of reaching equilibrium is much slower at low capillary pressures. In general, the porous plate method is considered to be the most accurate of the three methods, provided that adequate time is allowed to reach equilibrium. It can be used on heterogeneous or laminated samples.

And since the saturation distribution of the fluids at the end of each pressure step during the experiment are uniform throughout the sample, no interpretation model is needed (as when using the centrifuge method).

However, a porous plate experiment is much slower than the other methods. Typically, nearly a month may be required to reach equilibrium at each step.

- **Centrifuge**

The centrifuge technique¹⁴⁻²¹, for capillary pressure measurement on core samples, was introduced by Hassler and Brunner¹⁴ and Slobod *et al.*¹⁵ It requires two steps, the measurement of the centrifuge fluid production data and transformation of that data into capillary pressure curves. During the past decades, advances have been made in many aspects of centrifuge data processing. However, one has to keep in mind that it has not been perfected. Numerous publications claimed to provide improved solutions while later being corrected, and sometimes contradicted¹⁶⁻²¹

In the centrifuge technique, individual core plugs containing a high saturation of a single phase are mounted in coreholders and placed in a centrifuge. The plugs are in contact with a second fluid phase. Centrifugal force, applied by rotating the sample, generates a pressure gradient in each fluid phase that differs according to the fluid's density. As the first phase is produced from one end of the core plug, the second phase enters from the opposite end to replace it. The centrifuge speed is then increased stepwise and is maintained constant at each step until production ceases. The centrifuge method is faster than the porous plate, but not as fast as the mercury injection method. A typical equilibration time for each step is three to five days. But, tighter samples may require longer equilibration times. The centrifuge method is not recommended for heterogeneous or laminated rocks because the data analysis method may not accurately account for the distribution of fluids in a heterogeneous rock. Also, for highly permeable rocks, very limited data may be reliably collected at low capillary pressures.

- **Mercury Injection**

In the mercury injection technique²²⁻²³, a sample that has been extracted, dried, and evacuated is immersed in liquid mercury. Pressure is then increased stepwise, and the amount of mercury entering the sample is measured and converted to non-wetting phase saturation. Since mercury is strongly non-wetting in core material, these are drainage measurements. High mercury liquid - mercury vapor capillary pressure (5,000 – 70,000 psi) can be achieved to characterize the smallest pores, and the method can be applied to small and irregularly shaped rocks (e.g. drill cuttings). However, such measurements are usually made in the absence of net confining stress. The mercury injection method is the fastest of the three methods but it is still subject to errors associated with equilibration time. Adequate equilibration may require more than one day or as much as one week for full measurement of low quality rocks.

Only the mercury injection technique provides convenient measurement of entry pressure, the pressure at which the wetting phase begins to be displaced by the non-wetting phase.

The mercury injection technique may provide capillary pressure data as reliable as porous plate and centrifuge results, provided the samples are uniform, high quality rocks, and the tests are conducted under confining stress with adequate time allowed for equilibration. In fact, in such rare situations, all three techniques are expected to provide similar results. However, since mercury is not a reservoir fluid, the method may not replicate reservoir displacement processes accurately, particularly in the low saturation region.

Table 2.1 shows the advantages and disadvantages of the three commonly used techniques for drainage capillary pressure measurements.

Table 2.1 – Comparison of Different Techniques to Measure Capillary Pressure

	<i>Porous Plate</i>	<i>Centrifuge</i>	<i>Mercury Injection</i>
Advantages	<ul style="list-style-type: none"> - Most accurate - Heterogeneous / laminated samples - Can use stocktank oil at reservoir temperature - Combined p_c/R_t - Higher maximum p_c (up to 1000 psi) - Can use confining stress - No interpretation model needed because of uniform saturations - Can use whole core 	<ul style="list-style-type: none"> - Faster (weeks) - Better definition of low pressure p_c - Can use moderate confining stress - Can use stocktank oil at reservoir temperature (up to 150° F) 	<ul style="list-style-type: none"> - Fastest (days) - Very high p_c (70,000 psi, but without confining stress) - Moderate confining stress (but lower maximum p_c (5,000 psi)) - Can test heterogeneous samples - Can test irregularly Shaped rock (e.g., cuttings) - Better definition of entry pressure
Disadvantages	<ul style="list-style-type: none"> - Slow (months) - Can only use degassed fluids - Not a good measure of entry pressure, especially in high permeability rock 	<ul style="list-style-type: none"> - Not representative for heterogeneous rocks - Lower maximum p_c (up to 120 psi) - Interpretation model is needed because of non-uniform saturations - Severe centrifuge stress - Can only use degassed fluids - Not a good measure of entry pressure, especially in high permeability rock 	<ul style="list-style-type: none"> - Non-reservoir fluid - Sample contamination - May disturb delicate clays, if present - Not recommended for initial water saturation determination without validation by other methods

Capillary Models

Numerous models have been developed to simulate the capillary pressure responses of rocks and soils. Using fitting parameters, these capillary models are refined to allow for variations in sample properties, fluid type, and the interconnected nature of the void structure.

Corey²⁴ showed in 1954 that oil-gas capillary pressure curves can be expressed as:

$$\frac{1}{p_c^2} = CS_w^* \dots\dots\dots(2.5)$$

Where p_c is capillary pressure, C is a constant and S_w^* is the normalized wetting phase saturation.

In 1960, Thomeer²⁵ proposed an empirical relationship between capillary pressure and mercury saturation. He analyzed capillary pressure curves to define internal pore structure. He concluded that the shape of capillary curve depends on pore geometry.

$$p_c = p_e \left[\frac{S_{Hg}}{S_{Hg_\infty}} \right]^{-\frac{1}{F_g}} \dots\dots\dots(2.6)$$

Where p_e is the entry capillary pressure, S_{Hg} is the mercury saturation S_{Hg_∞} is the mercury saturation at an infinite capillary pressure, and F_g is the pore geometrical factor. Using a type curve approach, Thomeer constructed a family curves but no experimental data were shown.

In 1966, Brooks and Corey⁴ found a general for of capillary pressure function:

$$p_c = p_e (S_w^*)^{-1/\lambda} \dots\dots\dots(2.7)$$

Where λ is the pore size distribution index. This model is commonly used for consolidated porous media.

In 1980, Van Genuchten²⁶ adopted a capillary pressure model to predict the hydraulic conductivity of unsaturated soils. Van Genuchten model has advantages over the Brooks-Corey model. The Brooks-Corey model has a steep change in slope at the air entry pressure p_e .

$$S_w^* = \left[1 + \left[\frac{p_c}{p_e} \right]^n \right]^{-m} \dots\dots\dots(2.8)$$

The parameters m , n , and p_e are directly calculated using the slope of measured capillary pressure data. This model is commonly used for unconsolidated porous media

In 1998, Jin and Wunnik²⁷ proposed a capillary pressure model as:

$$p_c = p_c^0 \left[\left[\frac{d}{S_w - S_{wr}} \right]^n + a \right] \dots\dots\dots(2.9)$$

Where p_c^0 is the capillary pressure scaling factor, d is a constant to define the curvature, n is the asymmetry shape factor and a is a constant to control the value of the entry capillary pressure.

Different authors such as Li and Horne²⁸, Skelt and Harrison²⁹ and Lenormand³⁰ proposed other capillary pressure models under different conditions.

The common point with these models is that they are mostly empirical. The different parameters do not have usually physical significance. Nevertheless, Li proved that the Brooks and Corey model has a "solid theoretical basis" which explains why this model works well in many cases.

2.2 Definition of Permeability and Models

Definition

Permeability measurements in core samples are based on the observation that, under steady-state flowing conditions, the pressure gradient is constant and is directly proportional to the fluid velocity. This constant of proportionality, as defined by Darcy's law:

$$\frac{dp}{dx} = - \frac{\mu}{k} v_x \dots\dots\dots(2.10)$$

is the absolute core permeability, k .

Archie³¹ presented a conceptual model whereby all petrophysical properties could be "inter-related" — this is shown in **Fig. 2-4**, and we immediately note Archie's rationale — *i.e.*, volumetric properties are related to flow properties, but typically not completely. In viewing **Fig. 2-4** we can write the following functional relation for permeability by induction:

$$k = f(\text{porosity, composition, texture/sorting, structure, diagenesis... etc})$$

Porosity:

- Well Logs: Sonic, Density, Neutron, Resistivity, etc.

Composition: (Lithology)

- Well Logs: Gamma Ray, SP, Spectral Gamma Ray, Photoelectric, etc.
- Depositional Environment: Geological Description, Core/Cuttings, etc.

Texture/Sorting:

- Capillary Pressure: Displacement Pressure, Irreducible Saturation (from logs?), etc.
- Depositional Environment: Geological Description, Core/Cuttings, etc.

Structure: (Pore Structure)

- Grain Size Distributions.
- Gamma Ray/SP/Spectral Gamma Ray Logs, etc.
- Depositional Environment: Geological Description, Core/Cuttings, etc.

Diagenesis: (Alteration of Pore Structure)

- Compaction (core and well logs).
- Cementation (core only).
- Transformation of Minerals: V_{shale} (core and well logs), clay content (effect on ϕ and k)

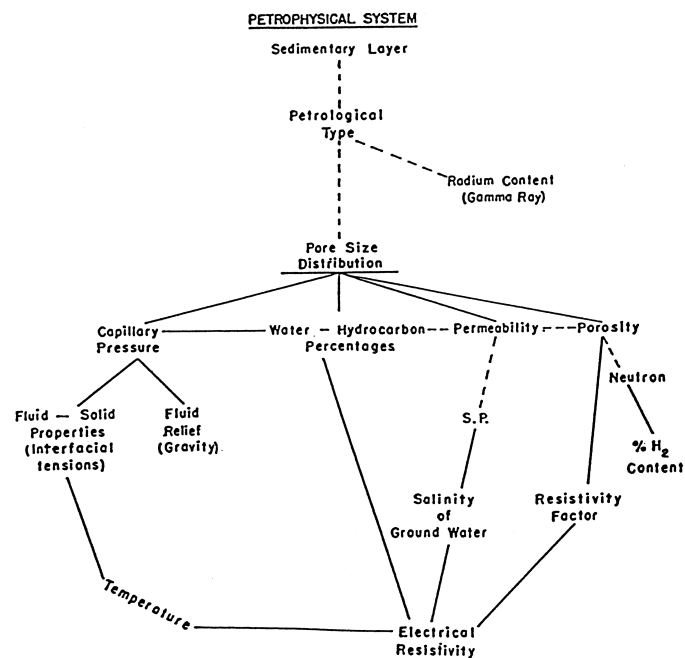


Figure 2.4 – Concept model for petrophysical systems as proposed by Archie.

The next major issue is not the "concept" of a correlation, but what variables can actually be correlated — again, returning to Archie³¹— we have correlation of permeability with porosity on a semilog (permeability scale). An example case provided by Archie (1950) is shown in **Fig. 2.5**. The value of Archie's contribution is not so much the accuracy of his proposals, but his emphasis on the underlying petrophysical relationships. While the logarithm of permeability is always correlated with porosity, there is no specific underlying theoretical/conceptual basis — only an observation that this concept works.

Variations on the concept of $k=a\exp(b\phi)$ (where a and b are arbitrary constants) as proposed by Archie include: Jennings and Lucia³² (2001) (**Fig. 2.6**), Cazier, *et al*³³ (1995) (**Fig. 2.7a**) and Berg³⁴(1970) (**Fig. 2.7b**). Where each of these works considers the "clean" sand case to be more of a power law (or direct proportionally) between porosity and permeability, and that "shaly" sands have some "non-power law" behavior, mostly the typical "exponential" model (*i.e.*, $\log(k)$ versus ϕ). These concepts essentially reinforce the empirical notion that a correlation of $\log(k)$ versus ϕ is the most relevant approach (in a practical sense). In short, we do not seek to disprove the $\log(k)$ versus ϕ concept — but rather, we will illustrate that this concept is simply a convenient representation of a (much) more complex process.

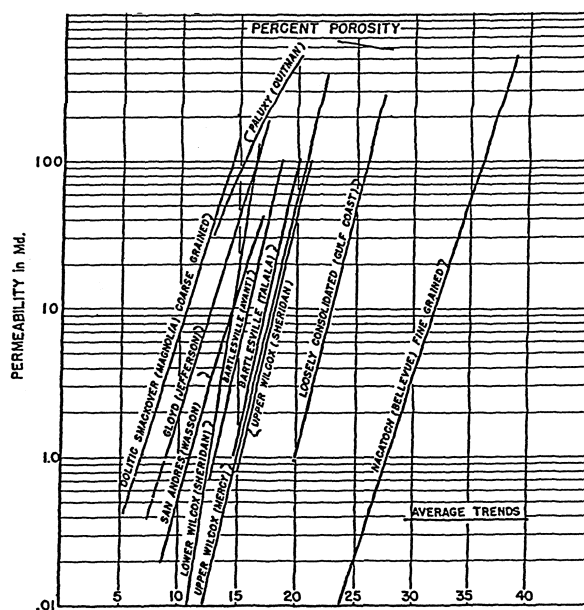


Figure 2.5 – Logarithmic (permeability) correlation proposed by Archie.

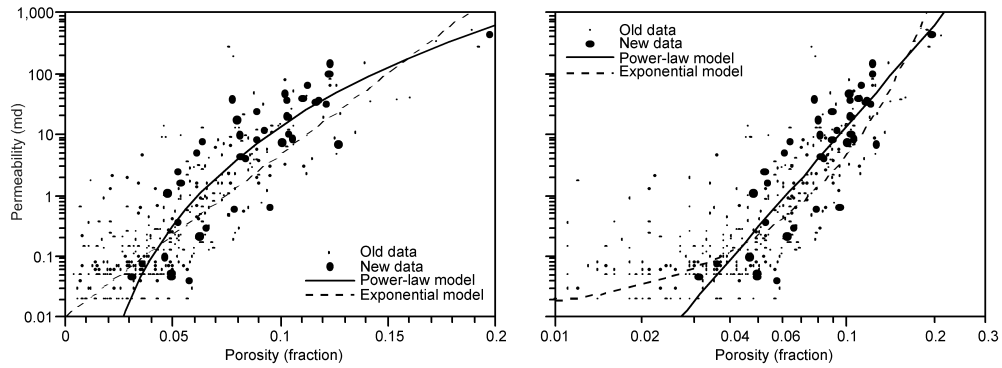


Figure 2.6 – Jennings and Lucia (concept) plot of clean and shaly sands — clean sand model: $k = \alpha \phi^\beta$ — shaly sand model: $k = a \exp(b \phi)$.

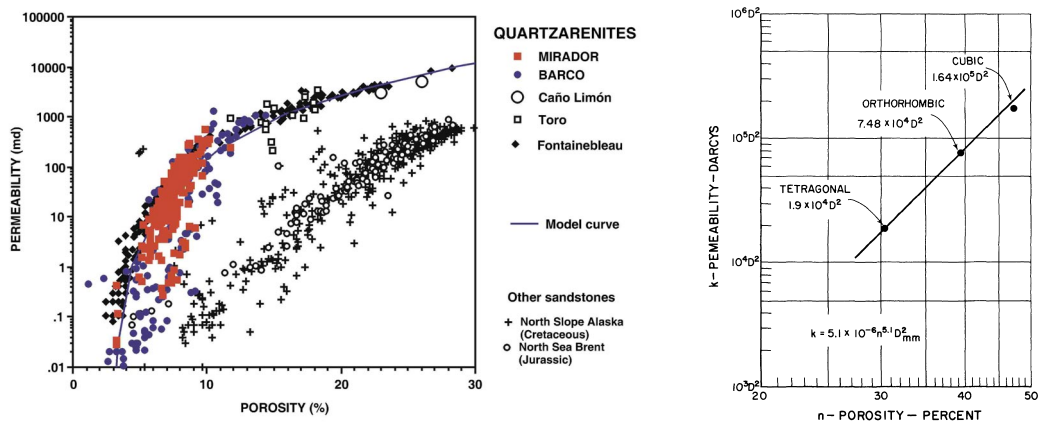


Figure 2.7 – **a.** Cazier, *et al* data for South American reservoir systems. **b.** Berg (1970) (idealized) power law model for permeability as a function of porosity and grain size.

Models of Permeability

The fundamental relationships between pore size/geometry and basic rock properties (*e.g.*, effective porosity, absolute permeability, *etc.*) are well-documented in the petroleum and petrophysics literature. Moreover, the literature is replete with models for estimating or predicting permeability from basic rock properties

• **Kozeny – Carman Model**

Kozeny³⁵ and Carman³⁶ related permeability with porosity and surface area of grains exposed to fluid flow for a tube like model of rock pore space. They proposed a simple relationship that states permeability is directly proportional to porosity and pore surface area per unit volume of rock. For randomly packed sphere, permeability is estimated as:

$$k = \frac{\phi^3}{f\tau A_g (1-\phi)^2} \dots\dots\dots (2.11)$$

Where ϕ is porosity, A_g specific surface area, and τ tortuosity. The technique is applicable to unconsolidated and synthetic porous media, from which the grain and pore properties could be characterized easily.

Archie³¹ proposed his well-known approach to quantifying the tortuosity term, the Kozeny-Carman equation become more useful for natural rock systems as:

$$k = \frac{r_{eff}^2}{8F} \dots\dots\dots (2.12)$$

Where r_{eff} effective pore radius and F formation factor.

• **Models Based on Grain Size and Mineralogy**

In 1943, Krumbein and Monk³⁷ measured permeability in sand packs with a constant porosity for specific size and sorting. Using experimental procedures, they obtained:

$$k = 760D_g^2 \exp(-1.3\sigma_D) \dots\dots\dots (2.13)$$

Where D_g is the geometric mean diameter in millimeter, σ_D is the standard deviation of grain diameter in phi units where $\phi = -\log [D(\text{mm})]$. Beard and Weyl³⁸ concluded this equation is valid for unconsolidated sand packs with a porosity range between 20 to 43 percent assuming that grain properties such as angularity sphericity and surface texture.

In 1970, Berg³³ presented a model linking grain size, shape and sorting to permeability:

$$k = 80.8\phi^{5.1}D^2e^{-1.385p} \dots\dots\dots (2.14)$$

Where D is the median grain diameter, ϕ is porosity in percent and p a sorting term. p is defined as $p = P_{90} - P_{10}$. Nelson³⁹ tested Berg's model validity with three different data sets (sandstones, carbonates). His conclusions are that *Berg's model appears to be usable means of estimating permeability in unconsolidated sands and relatively clean consolidated quartzose rocks* for porosity greater than 30 percent.

In 1979, Van Baaren⁴⁰ used an empirical approach to obtain the following model:

$$k = 10D_d^2\phi^{3.64+m}C^{-3.64} \dots\dots\dots (2.15)$$

Where D_d (μm) is the dominant grain size form petrological observation and C is a sorting index given by the **Table 2.2**.

Table 2.2 – Van Baaren Empirical Data

<i>Sorting</i>	<i>C</i>	<i>D_{max}/D_{min}</i>
Extremely well to very well sorted	0.70	2.5
Very well to well	0.77	–
Well	0.84	3.5
Well to moderately	0.87	–
Moderately	0.91	8
Moderately to poorly	0.95	–
Poorly	1.00	–

• **Models Based on Surface Area and Water Saturation**

Wyllie and Rose⁴¹ proposed a modification to the Kozeny and Carman equation and substituted irreducible water saturation for specific surface area. They assumed that irreducible water saturation is related to specific surface area. The resulting equation is:

$$k = \left[B \frac{\phi^3}{S_{wir} - B'} \right]^{\frac{1}{2}} \dots\dots\dots (2.16)$$

Where B is a coefficient related to hydrocarbon type and gravity, B' is a correction factor for data fitting.

Timur⁴² proposed a generalized equation in the form:

$$k = A \frac{\phi^B}{S_{wi}^C} \dots\dots\dots (2.17)$$

That can be evaluated in terms of the statistically determined parameters A , B , and C . He applied a reduced major axis method of analysis to data obtained by laboratory measurements conducted on 155 sandstone samples from three different oil fields from North America. Based both on the highest correlation coefficient and on the lowest standard deviation, Timur has chosen from five alternative relationships the following formula for permeability.

$$k = 0.136 \frac{\phi^{4.4}}{S_{wi}^2} \dots\dots\dots (2.18)$$

In practice, the correlation can be very poor between measured and estimated permeability. Adjustment of parameters A , B , and C can improve the correlation.

An extension of the equation 2.15 is made by Coates⁴³. It allows that permeability goes to zero as S_{wi} increases to fill the entire pore space.

$$k = \left[\frac{100\phi_e^2(1-S_{wi})}{S_{wi}} \right]^2 \dots\dots\dots (2.19)$$

• Models Based on Nuclear Magnetic Resonance

There are two widely accepted models in the literature for estimating permeability using NMR data: the Free Fluid model and the Mean T_2 model. These two methods both express permeability as a function of porosity. Porosity is governed by the size of the pore bodies, as the spaces between grains formulate porosity. Permeability, however, is controlled by the pore throats. Many researchers have found that pore size distributions obtained from NMR and pore throat distributions are in fact very similar in shape, at least for sandstones. This is because in simple geometry sandstones, the relationship between pore bodies and throats is relatively constant, so pore body distributions can be used as an approximation for the pore throat distributions. Empirical constants are introduced in the models to shift the pore body distributions measured with NMR to the pore throats. In this manner, porosity and permeability can be strongly related.

The Free Fluid model was developed by Coates. In this model, permeability is estimated by:

$$k = \left[\left[\frac{\phi}{C} \right]^2 \left[\frac{\text{FFI}}{\text{BVI}} \right] \right] \dots\dots\dots (2.20)$$

Where C is empirical constant FFI the free flow index (the fractional part of formation volume occupied by fluids that are free to flow); obtained by summing the T_2 distribution over T_2 values greater than $T_{2cutoff}$ and BVI the bound volume of irreducible water.

The SDR model was developed originally in 1988 in terms of T_1 , and that version has been modified to become the SDR (Schlumberger-Doll Research) model in 1998:

$$k = aT_{2gm}^2 \phi^4 \dots\dots\dots (2.21)$$

Where a is a coefficient that depends on the formation type, T_{2gm} the geometric mean T_2 of the spectrum.

Many researchers have observed that these two models of estimating permeability do not work well for every formation. Instead, they have proposed alternative methods of estimating permeability.

In 2000, Rodrigues *et al.*⁴⁴ proposed that the short times of T_2 spectra correspond to the transport properties of the rock, thus permeability estimation should only include early times. They state that when the geometric mean T_2 for the entire spectrum is used, a lot of the information is lost.

In 1999, Quintero *et al.*⁴⁵ have also attempted to develop an NMR permeability model for use in a logging tool. They provide modifications of the SDR method as follows:

$$k = Cpf 4.6\phi^4 T_{2lm}^2 \dots\dots\dots (2.22)$$

Where $pf = 10^{(2width_l / t2width_m)}$; width of T_2 distribution at a specific depth interval (t_{2width}) and the width of the T_2 distribution in a mud-supported facies.

• **Models Based on Fractal Dimension**

The microscopic properties of the rocks, such as specific surface area, throat size, grain size, and tortuosity, are commonly used in relating permeability to the fractal dimension of those properties⁴⁶⁻⁵³. These studies used different types of sandstones or synthetic porous media to develop or verify the fractal permeability correlations. The fractal models for permeability are listed in **Table 2.3**.

Table 2.3 – Fractal Models

Model	Equation	Variables other than porosity
Katz and Thomson ⁴⁶ (1986)	$k = \frac{1}{226} l_c^2 \frac{\sigma}{\sigma_o}$	Some characteristic length of pore space (l_c), conductivity of water (σ_o) and conductivity of water saturated rock (σ).
Mavko and Nur ⁴⁷ (1997)	$k \propto c(\phi - \phi_c)^3 d^2$	Particle size, threshold porosity, particle size.
Martys <i>et al.</i> ⁴⁸ (1994)	$k = \frac{2\phi_2^*}{s^2} (\phi_1 - \phi_1^c)^f$ $k = k_o (\phi_1 - \phi_1^c)^g$	Specific surface area, threshold porosity; $g=4, f=4.2$.
Pape <i>et al.</i> ⁴⁹ (1999)	$k = A\phi + B\phi^{\text{exp1}} + C(10\phi)^{\text{exp2}}$	$\text{exp}_1 = m$ (Archie's constant). $\text{exp}_2 = m + 2/[c_1(3-D)]$, $0.39 < c_1 < 1$
Muller and McCauley ⁵⁰ (1992)	$k \propto \phi^{(4-D)/D}$	Fractal dimension
Wong ⁵¹ (1988)	$k = \frac{c_1 l_g^2}{F} \text{ and } k = \frac{c_2 l_t^2}{F}$	Formation factor, characteristic grain size (l_g), and characteristic throat size (l_t)
Hansen and Skjeltorp ⁵² (1988)	$k_r = c' \phi (l_1 / l_n)^2 [(E_s - D_s) - (D_v - E_v)]$	Characteristic length, euclidean dimensions and fractal dimension
Garrison <i>et al.</i> ⁵³ (1993)	$k = 10^{-1.7 - 0.6 D'_{S(\text{control})} + 113 S'_{a(\text{control})}}$	Apparent surface fractal dimension and area shape factor

• **Models Based on Pore Dimension**

Leverett J-Function ($J(S_w)$)

One of the first correlation models for petrophysical properties was proposed by Leverett⁵⁴ who developed a relationship between wetting phase saturation and the interfacial curvature between the wetting and non-wetting fluids in the pore throats (this relationship is based primarily on a dimensional balance of the parameters (e.g., $\sqrt{k/\phi}$ is an "equivalent length")). This concept (i.e., the "J-function") was proposed by Leverett as a dimensionless function that could be used to normalize capillary pressure data for a range of rock properties.

The Leverett J-function is defined as

$$J(S_w) = \frac{P_c}{\sigma \cos \theta} \sqrt{k/\phi} \dots\dots\dots (2.23)$$

where:

- k = permeability, cm² (1 D = 9.86923x10⁻⁹ cm²)
- $J(S_w)$ = dimensionless capillary pressure-saturation function
- σ = interfacial tension, dynes/cm
- θ = contact angle of incidence for wetting phase, radians
- ϕ = porosity, fraction of pore volume
- S_w = wetting phase saturation, fraction of pore volume
- p_c = capillary pressure, dynes/cm²
- $\sqrt{k/\phi}$ = equivalent length, cm

Purcell Permeability Relation

In 1949, Purcell¹ developed an equation relating absolute permeability to the area under the capillary pressure curve generated from mercury injection. We note that Purcell's equation *assumes that fluid flow can be modeled using Poiseuille's Law where the rock pore system is represented by a bundle of parallel (but tortuous) capillary tubes of various radii*. Further, the range of tube radii are characterized by the pore size distribution as computed from the area under the capillary pressure curve.

Purcell's original permeability model is given by:

$$k = 10.66 (\sigma_{Hg-air} \cos \theta)^2 F_P \phi \int_0^1 \frac{1}{P_c^2} dS_w \dots\dots\dots (2.24)$$

where:

- k = permeability, md
- 10.66 = units conversion constant, md-(psia)²/(dynes/cm)²
- F_p = Purcell lithology factor, dimensionless
- σ_{Hg-air} = mercury-air interfacial tension, dynes/cm
- θ = contact angle of incidence for wetting phase, radians
- ϕ = porosity, fraction of pore volume
- S_w = wetting phase saturation, fraction of pore volume
- p_c = capillary pressure, psia

We note that F_p is the Purcell "lithology factor" which is used to represent the differences between the hypothetical model and actual rock pore system. The F_p "lithology factor" is an empirical correction that Purcell determined for several different core samples over a range of absolute permeability values.

Rose and Bruce Study

In 1949, Rose and Bruce¹³ conducted a sensitivity study of rock properties and their impact on the shape of mercury-injection capillary pressure curves. They showed that the measured capillary pressure depends on pore configuration, rock surface properties and fluid properties. Rose and Bruce also found that capillary pressure curves can be used to characterize the distribution, orientation, shape and tortuosity of the pore system — as well as the interfacial and interstitial surface area. Although Rose and Bruce did not propose a permeability relation, they did demonstrate the use of the Leverett J -Function (Eq. 2-23) (with extensions of their own) to generate relative permeability-saturation profiles.

Calhoun Permeability Relation

In 1949, Calhoun, *et al*⁵⁵ showed that the Purcell¹ lithology factor (F_p) is inversely proportional to the formation tortuosity factor (τ). Their study also determined that the internal rock surface area could be defined in terms of the fluid interfacial tension, rock-wetting phase fluid contact angle, and the area under the capillary pressure curve. Additionally, Calhoun, *et al* developed a semi-empirical relationship for absolute permeability as a function of effective porosity, adhesive tension, capillary displacement pressure, and the value of the J -Function at 100 percent wetting phase saturation. Calhoun, *et al*⁵⁵ semi-empirical relationship is given as:

$$k = \frac{1}{P_d^2} [J(S_w)_{1.0}]^2 (\sigma \cos \theta)^2 \phi \dots\dots\dots (2.25)$$

where:

- k = permeability, cm² (1 D = 9.86923x10⁻⁹ cm²)
- $J(S_w)_{1.0}$ = dimensionless capillary pressure function at $S_w=1.0$
- σ = interfacial tension, dynes/cm
- θ = contact angle of incidence for wetting phase, radians
- ϕ = porosity, fraction of pore volume
- S_w = wetting phase saturation, fraction of pore volume
- p_d = capillary displacement pressure, dynes/cm²

We note that **Eq. 2.25** was *validated* by Calhoun, *et al* only for high permeability rocks.

Burdine Permeability Relation

In 1950, Burdine *et al*² extended the Purcell¹ model for a bundle of capillary tubes and showed that the absolute permeability of a particular rock is a function of pore entry radii and the mercury-filled pore volume. The Burdine equation is given by:

$$k = 126 \phi \sum_{i=0}^n \frac{V_i \bar{R}_i^{-4}}{X_i^2 \bar{R}_i^2} \dots\dots\dots (2.26)$$

where:

- k = permeability, md (1 D = 9.86923x10⁻⁹ cm²)
- 126 = units conversion constant (Poiseuille → Darcy units)
- V_i = incremental pore volume filled by mercury, cm³
- R_i = incremental pore entry radius, cm
- \bar{R}_i = average pore entry radius, cm
- X_i = tortuosity factor ($X_i=L_i/L_{tot}$), fraction
- L_i = effective length of flow path, cm
- L_{tot} = actual length of flow path, cm

We note that the *Burdine et al* relation is fundamentally similar (in derivation) to the Purcell relation — the interested reader is also directed to an additional reference article⁵⁶ by *Burdine et al* where additional detail and clarity of nomenclature are provided for **Eq. 2.26**.

Wyllie-Spangler Permeability Relation

In 1952, Wyllie and Spangler⁴¹ developed a model using the Purcell/Burdine concept, but Wyllie and Spangler used electric log properties to determine the tortuosity factor (specifically, this is given in terms of the *formation factor* which is defined as the ratio of the resistivity of the formation at 100 percent wetting phase saturation to the resistivity of the formation brine).

The Wyllie-Spangler equation, which relates absolute permeability to mercury-injection capillary-pressure curve proper-ties, is given by

$$k = 10.66 (\sigma_{Hg-air} \cos \theta)^2 \frac{1}{F_{WS}} \frac{1}{F^2 \phi} \int_0^1 \frac{1}{p_c^2} dS_w \dots\dots\dots (2.27)$$

where F is the Archie³¹ formation factor, defined by

$$F = \frac{a}{\phi^m} = \frac{R_o}{R_w} \dots\dots\dots (2.28)$$

where:

- k = permeability, md
- 10.66 = units conversion constant, md-(psia)²/(dynes/cm)²
- F_{WS} = Wyllie-Spangler shape factor, dimensionless
- θ = contact angle of incidence for wetting phase, radians
- ϕ = porosity, fraction of pore volume
- S_w = wetting phase saturation, fraction of pore volume
- p_c = capillary pressure, psia
- F = Archie formation factor, dimensionless
- R_o = resistivity of formation at $S_w=1.0$, ohm-m
- R_w = resistivity of formation brine, ohm-m
- m = empirical constant (*cementation factor*), dimensionless
- a = empirical constant, dimensionless

In Eq. 2.28, a is an *empirical constant* (a is often assumed to be 1) and m is the *cementation factor* (m is often assumed to be 2) Note that m is a function of pore type, pore geometry and lithology. Wyllie and Spangler also demonstrate that the tortuosity factor can be related to the formation factor deter-mined from electric log measurements (Wyllie and Spangler actually made their developments in terms of the tortuosity factor, then "converted" their result into a formulation which uses the formation resistivity factor).

Thomeer Permeability Relation

In 1960, Thomeer²⁵ observed that a log-log plot of capillary pressure could be approximated by a hyperbola. *Thomeer described the hyperbola location on the x-y coordinate system by the position of the two end-point curve asymptotes, and he defined the extrapolated asymptotes on the x- and y-axes as the displacement pressure and the bulk volume occupied by mercury at an infinite pressure, respectively.*

In addition, Thomeer hypothesized that the shape of the hyperbola reflects the pore geometry, so he used the curve shape to define a pore geometrical factor. We note that Thomeer assigned the pore geometric factor a value between 0 and 10, where low values represent large well-sorted pore openings and high values represent high levels of variation in pore opening sizes. As a result of these definitions, Thomeer proposed an empirical equation relating air permeability to capillary pressure, displacement pressure, non-wetting phase saturation, and pore geometric factor.

The Thomeer model is given as:

$$\frac{S_b}{S_{b\infty}} = e^{-F_g / [\log(p_c/p_d)]} \dots\dots\dots (2.29)$$

where:

- k = permeability, md
- p_c = capillary pressure, psia
- p_d = capillary displacement pressure, psia
- S_b = Hg saturation, fraction of *bulk* volume
- $S_{b\infty}$ = Hg saturation at $p_c = \infty$, fraction of *bulk* volume
- F_g = pore geometrical factor, dimensionless

Using laboratory measurements from 165 sandstone and 114 carbonate samples, Thomeer⁵⁷ formulated the following equation that relates absolute permeability to effective porosity, capillary displacement or threshold pressure, and the pore geometric factor:

$$k = 3.8068 F_g^{-1.3334} \left[\frac{S_{b\infty}}{P_d} \right]^2 \dots\dots\dots (2.30)$$

Swanson Permeability Relation

As a follow-up effort to Thomeer,²⁵⁻⁵⁷ Swanson⁵⁸ developed an equation to compute absolute permeability based on specific capillary pressure curve characteristics. The form of Swanson's equation is: (using the same nomenclature as Thomeer):

$$k = a_1 \left[\frac{S_b}{p_c} \right]_A^{a_2} \dots\dots\dots (2.31)$$

where:

k = permeability, md

$[S_b/p_c]_A$ = Hg saturation/capillary pressure "apex," fraction/psia

A = "apex" point on $\log(p_c)$ vs. $\log(S_b)$ curve at which a 45° line becomes tangent

The subscript "A" (or apex) refers to the maximum ratio of the mercury saturation to the capillary pressure. Swanson hypothesized that the maximum ratio occurs at the point at which all of the major connected pore space is filled with mercury. Further, the capillary pressure at the apex reflects the dominant interconnected pores and pore throats controlling most of the fluid flow characteristics.

The constants a_1 and a_2 in Eq. 2.31 represent various rock lithologies and fluid types, respectively, in the system. Swanson used regression analysis and correlated the constants in Eq. 2.31 with properties from 203 sandstone samples from 41 formations and 116 carbonate samples from 330 formations. The best fit of the air permeability data was obtained with

$$k = 389 \left[\frac{S_b}{p_c} \right]_A^{1.691} \dots\dots\dots (2.32)$$

Wells and Amaefule Permeability Relation

In 1985, Wells and Amaefule⁵⁹ modified the Swanson approach for low-permeability or "tight gas sands." Wells and Amaefule found that by plotting the logarithm of mercury saturation (S_b , percent of bulk volume) against the square root of capillary pressure-mercury saturation ratio (S_b/p_c), they could observe a well-defined minimum — which represents the inflection point of the capillary pressure curve. Consequently, (S_b/p_c) could be calculated as the inverse of the squared minimum value. Wells and Amaefule then correlated the Swanson⁵⁸ parameter with air permeabilities for 35 low-permeability sandstone samples and developed the following equations for calculating absolute permeability:

$$k = 30.5 \left[\frac{S_b}{p_c} \right]_{A,Hg-air}^{1.56} \dots\dots\dots (2.33a)$$

$$k = 1.22 \left[\frac{S_b}{p_c} \right]_{A,brine-air}^{1.61} \dots\dots\dots (2.33b)$$

where:

k = permeability, md

p_c = capillary pressure, psia

S_b = non-wetting saturation, fraction of *bulk* volume

$[S_b/p_c]_A$ = non-wetting saturation/cap. pressure "apex," fraction/psia

A = "apex" point on $\log(p_c)$ vs. $\log(S_b)$ curve at which a 45° line becomes tangent

Winland Permeability Relation

A methodology attributed to Winland (no reference other than company) was documented initially by Kolodzie⁶⁰ and extended by Pittman⁶¹ where regression analysis was used to develop an empirical relationship that is *conceptually* similar to Swanson.⁵⁸ The "Winland" equation describes the relationship for absolute permeability, effective porosity, and a capillary pressure parameter (R_{35}) as follows:

$$\log R_{35} = 0.732 + 0.588 \log k - 0.864 \log \phi \dots\dots\dots (2.34)$$

where:

k = permeability, md

ϕ = porosity, fraction of pore volume

R_{35} = pore throat radius at an Hg saturation of 35 percent, μm

R_{35} is the capillary pressure parameter used in the Winland study — specifically, R_{35} is the pore throat radius (in μm) at a mercury saturation of 35 percent, where this value is a function of both pore entry size and the sorting of pore throat sizes. According to Nelson,³⁹ the R_{35} parameter quantifies the largest and best-connected pore throats. We note from refs. 61-62 that other capillary pressure parameters (*i.e.*, R_{30} , R_{40} and R_{50} values) were considered, but the R_{35} capillary pressure curve parameter provided the best statistical fit.

The Winland data set includes 56 sandstone and 26 carbonate samples with permeability measurements corrected for gas slippage or Klinkenberg⁶² effects. This data set also includes another 240 samples of various lithologies but without permeabilities corrected for gas slippage effects. *We note that the permeability computed by Eq. 2. is not the Klinkenberg-corrected permeability.*

CHAPTER III

DEVELOPMENT OF A SEMI-ANALYTICAL ESTIMATE OF PERMEABILITY OBTAINED FROM CAPILLARY PRESSURE

3.1 Development and Validation of New Model

The foundations of our correlation model are the classic Purcell¹ and Burdine² equations — which assume that the porous medium can be modeled as a bundle of parallel (but tortuous) capillary tubes of various radii. Further, the range of tube radii are characterized by the pore size distribution as computed from the area under the capillary pressure curve.

The classic Purcell-Burdine k -model has been re-derived by Nakornthap and Evans⁶³ — and this "redevelopment" includes considerations by Wyllie and Spangler⁴¹ and Wyllie and Gardner.³

The final form of the Nakornthap and Evans result, solved for formation permeability, is given as:

$$k = 10.66 \frac{\omega}{n} \frac{1}{2} (\sigma_{Hg-air} \cos \theta)^2 (1 - S_{wi})^3 \phi^3 \int_0^1 \frac{1}{p_c^2} dS_w^* \dots \dots \dots (3.1)$$

where: (written for an Hg-air system (*i.e.*, $S_w = S_{air}$))

- k = permeability, md
- 10.66 = units conversion constant, md-(psia)²/(dynes/cm)²
- ω = pore throat "impedance" factor, dimensionless
- n = number of entrances/exits in a pore, dimensionless
- σ_{Hg-air} = mercury-air interfacial tension, dynes/cm
- θ = contact angle of incidence for wetting phase, radians
- ϕ = porosity, fraction of pore volume
- p_c = capillary pressure, psia
- S_w = wetting phase saturation, fraction of pore volume
- S_{wi} = irreducible wetting phase saturation, fraction of pore volume
- S_w^* = $(S_w - S_{wi}) / (1 - S_{wi})$, "effective" (or normalized) wetting phase saturation function, dimensionless

The definition of the "effective" (or normalized) wetting phase saturation function was first proposed by Burdine² and later utilized directly by Wyllie and Gardner.³ This definition is given as:

$$S_w^* = \frac{S_w - S_{wi}}{1 - S_{wi}} \dots\dots\dots (3.2)$$

In this approach, we incorporate the capillary pressure curve characteristics using the Brooks-Corey³ power-law model which is given by:

$$p_c = p_d \left[\frac{S_w - S_{wi}}{1 - S_{wi}} \right]^{-\frac{1}{\lambda}} \dots\dots\dots (3.3)$$

where: (writing for an Hg-air system (*i.e.*, $S_w = S_{air}$))

- p_c = capillary pressure, psia
- p_d = displacement pressure, psia
- S_w = wetting phase saturation, fraction of pore volume
- S_{wi} = irreducible wetting phase saturation, fraction of pore volume
- λ = Brooks-Corey index of pore-size distribution, dimensionless

Where p_d is the capillary displacement (or threshold) pressure, and λ is the index of pore-size distribution. Combining Eqs. 3.1-3.3 yields the basic form of the permeability equation used in our study:

$$k = 10.66 \frac{\omega}{n} (\sigma_{Hg-air} \cos \theta)^2 (1 - S_{wi})^3 \phi^3 \frac{1}{p_d^2} \left[\frac{\lambda}{\lambda + 2} \right] \dots\dots\dots (3.4)$$

While we could not find the explicit form given by Eq. 3.4 in the literature, it has undoubtedly been derived as Eq. 16 is the generalized formulation used to derive the relative permeability relations of Brooks and Corey³ the results of which are also presented by Nakornthap and Evans.⁶³

Nakornthap and Evans assign the ω and n parameters to address non-ideal flow behavior. To describe the ω -parameter, Nakornthap and Evans state:

The ω -parameter is inserted to recognize the fact that flow through a pore of radius r overemphasizes the impedance because it ignores the larger areas available for exit-flow at either side of the constrictions formed where pores abut. Thus it may be expected that $\omega \geq 1$ and that the actual magnitude of ω is a function of the average shape of pores in the medium that the model represents. ω is assumed constant for all pore sizes.

Similarly, Nakornthap and Evans describe the n -parameter, as follows:

The numerical constant n reflects the manner in which the available interconnecting pore area is divided. In the most favorable case for flow, all the exit area is concentrated in one pore; then $n = 1$. It may be expected, therefore, that $n \geq 1$. It is assumed here that n is constant for all pore sizes.

Ali⁶ has also suggested the following concept models for representing ω and n :

$$\omega = \frac{1}{\phi} \dots\dots\dots (3.5)$$

$$n = \frac{1}{(1 - S_{wi})} \dots\dots\dots (3.6)$$

Substituting Eqs. 3.5 and 3.6 into Eq. 3.4, we can eliminate the ω and n terms directly, which yields:

$$k = 10.66 \alpha (\sigma_{Hg-air} \cos \theta)^2 (1 - S_{wi})^4 \phi^2 \frac{1}{p_d^2} \left[\frac{\lambda}{\lambda + 2} \right] \dots\dots\dots (3.7)$$

Note that we have added an empirical parameter, α , in Eq. 19 to represent any remaining non-idealities that have not been accounted for by any other terms. If we were to attempt to utilize Eq. , we would likely assume $\alpha = 1$, or attempt a calibration of the α -parameter for a particular data set. In fact, we did use Eq. 3.7 in some of our early correlation efforts as a "test function," where we plotted permeability computed using Eq. 3.7 versus measured permeability on a log-log plot to assess significant outlying data.

Perhaps the most significant contribution of this work will be presentation of Eq. 3-4 — as this relation clearly states that permeability should be a power law function of displacement pressure, index of pore-size distribution, irreducible wetting phase saturation, and porosity. Recasting Eq. 3-4 as a power law correlation model gives us:

$$k = a_1 \frac{1}{(p_d)^{a_2}} \left[\frac{\lambda}{\lambda + 2} \right]^{a_3} (1 - S_{wi})^{a_4} \phi^{a_5} \dots\dots\dots (3.8)$$

where a_1 , a_2 , a_3 , a_4 , and a_5 are correlation constants — coefficient a_1 incorporates all of the "constant" terms (*i.e.*, 10.66, ω/n , and $(\sigma_{Hg-air} \cos(\theta))^2$).

The form of Eq. 3.8 (or a simplified modification) permits us to create other relations — specifically, we can make model substitutions for other parameters (in our case, p_d and λ) and create a "universal" (albeit simplified) model for permeability based solely on porosity (ϕ) and irreducible wetting phase saturation (S_{wi}). This effort is presented in Appendix E.

We also utilize the power-law model form as a mechanism to correlate the displacement pressure (p_d). In this case, we correlate the displacement pressure (p_d) in terms of permeability, porosity and irreducible wetting phase saturation using:

$$p_d = b_1 \phi^{b_2} k^{b_3} (1 - S_{wi})^{b_4} \dots\dots\dots (3.9)$$

where b_1 , b_2 , b_3 , and b_4 are correlation parameters for the capillary displacement (or threshold) pressure. This effort is presented in Appendix F.

Lastly, we correlate the "index of pore-size distribution" (λ) with permeability, porosity, irreducible wetting phase saturation and capillary displacement pressure, again using a power-law model. This formulation is given as:

$$\lambda = c_1 \phi^{c_2} k^{c_3} (1 - S_{wi})^{c_4} p_d^{c_5} \dots\dots\dots (3.10)$$

where c_1 , c_2 , c_3 , c_4 , and c_5 are correlation parameters for the pore geometric factor. (Appendix G)

To calibrate the proposed power models (Eq. 3.8-3.10), we have used mercury-injection capillary-pressure data from the literature^{1,3,31} and industry sources. Furthermore, we have tested our new model using samples from both sandstone and carbonate lithologies. Although we did not evaluate a range of different carbonate rock types, we expect our new model to be most applicable to carbonates with an inter-granular type of porosity and not "vuggy" carbonates.

We reviewed approximately 120 data sets — but used only 89 data sets in this work. The data not used in this study were set aside for a variety of reasons (*i.e.*, suspicious character in the capillary pressure data (*e.g.*, "double porosity" behavior), erroneous capillary data (poor calibration, poor character), and we also used only Hg-air capillary pressure data — so air-oil, and oil-water data were set aside for later studies).

The data sets used in our correlations have the following ranges of properties:

$$\begin{aligned} 0.0041 &< k < 8340 \text{ md} \\ 0.003 &< \phi < 0.34 \text{ (fraction)} \\ 0.007 &< S_{wi} < 0.33 \text{ (fraction)} \\ 2.32 &< p_d < 2176 \text{ psia} \end{aligned}$$

3.2 Results and Discussion

Estimation of p_d , S_{wi} and λ from Regression

Our initial calibration process was performed to estimate the capillary displacement pressure (p_d), irreducible wetting-phase saturation (S_{wi}), and the index of pore-size distribution (λ) on a sample-by-sample basis using Eq. 3.3 (*i.e.*, the Brooks-Corey $p_c(S_w)$ model).

We could have attempted a "global" calibration of the p_d , S_{wi} and λ parameters simultaneously with the model parameters in Eqs. 3.8-3.10. Such a process would (in concept) be more robust — *i.e.*, coupling the calibration of the Brooks-Corey model with each of the regression models (Eqs. 3.8-3.10). However, the quality of data, coupled with the bias (human intervention) required to properly fit the Brooks-Corey $p_c(S_w)$ model to an individual sample data set, required that we perform this calibration separately. The results of the p_d , S_{wi} and λ calibration, along with the input permeability (k) and porosity (ϕ) data for this work are summarized in Appendices I-M.

In **Fig. 3.1** we present a typical $p_c(S_w)$ data-model regression to illustrate our calibration process. We clearly note that, while the data-model fit is good, human intervention is required to ensure that the model is properly applied to the data.

Determination of the λ -parameter is sometimes difficult. **Figs. 3.2 – 3.4** show the method used in this study. λ -parameter in Fig 3-2 is determined as the slope of the curve. Fig 3.3 and Fig 3.4 are type curves to determine λ -parameter.

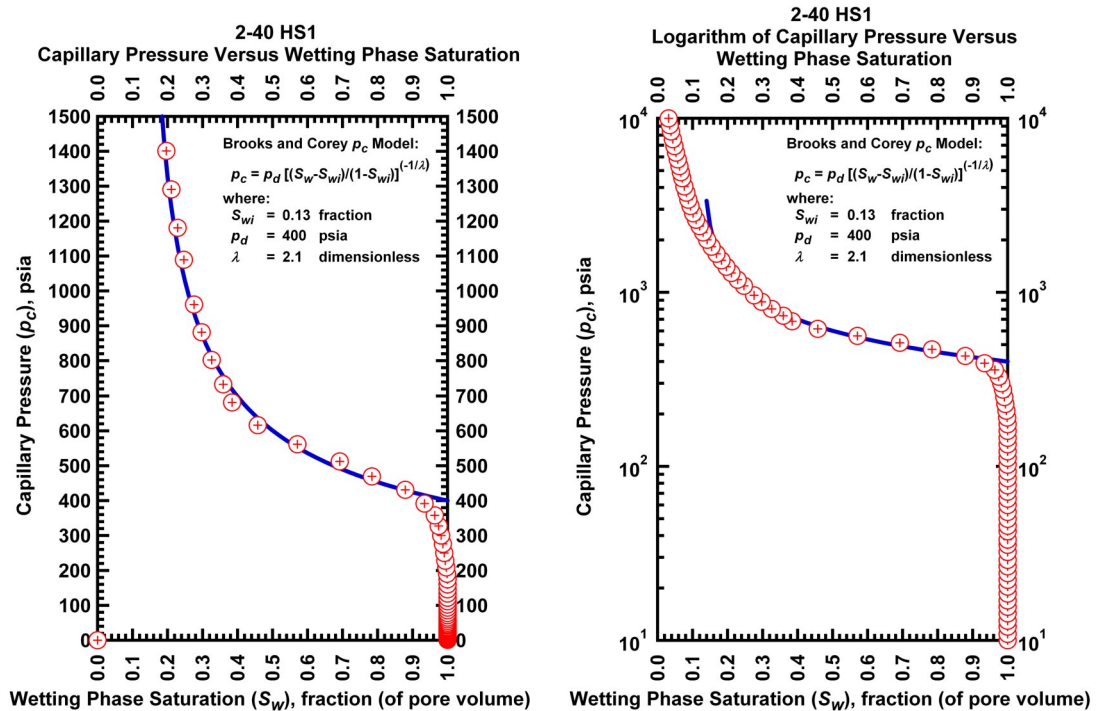


Figure 3.1 – Example correlation of Brooks-Corey $p_c(S_w)$ model to a typical core data set for this study **a.** Capillary pressure versus wetting phase saturation plot – Cartesian capillary pressure format. **b.** Capillary pressure versus wetting phase saturation plot – Logarithmic capillary pressure format.

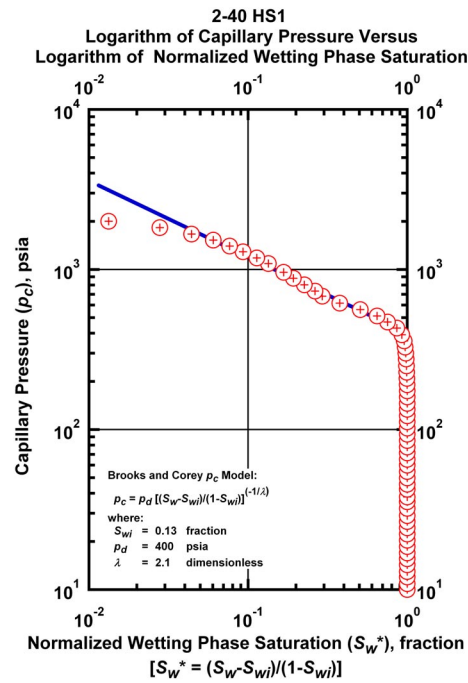


Figure 3.2 – Capillary pressure versus normalized wetting phase saturation plot – Cartesian capillary pressure format.

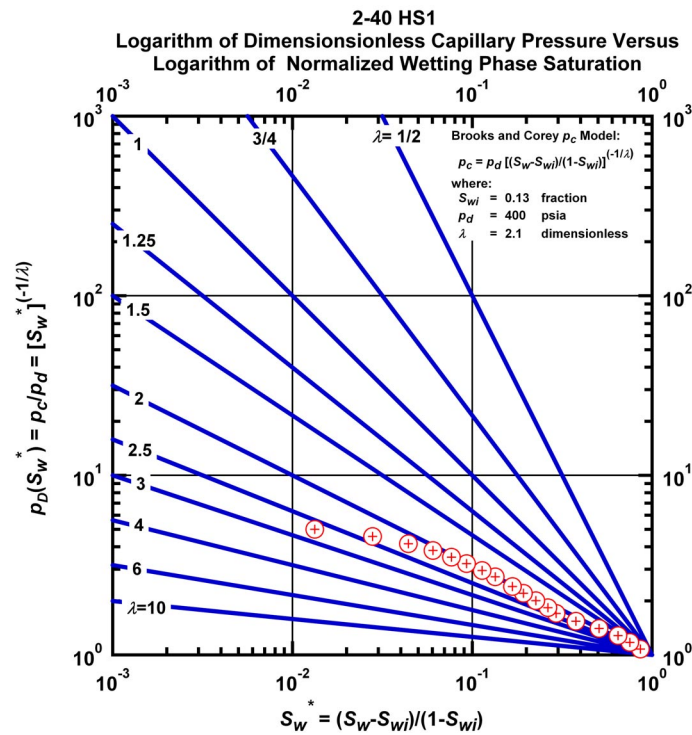


Figure 3.3 – Dimensionless capillary pressure versus normalized wetting phase saturation plot – Log-Log format "Type curve" for capillary pressure.

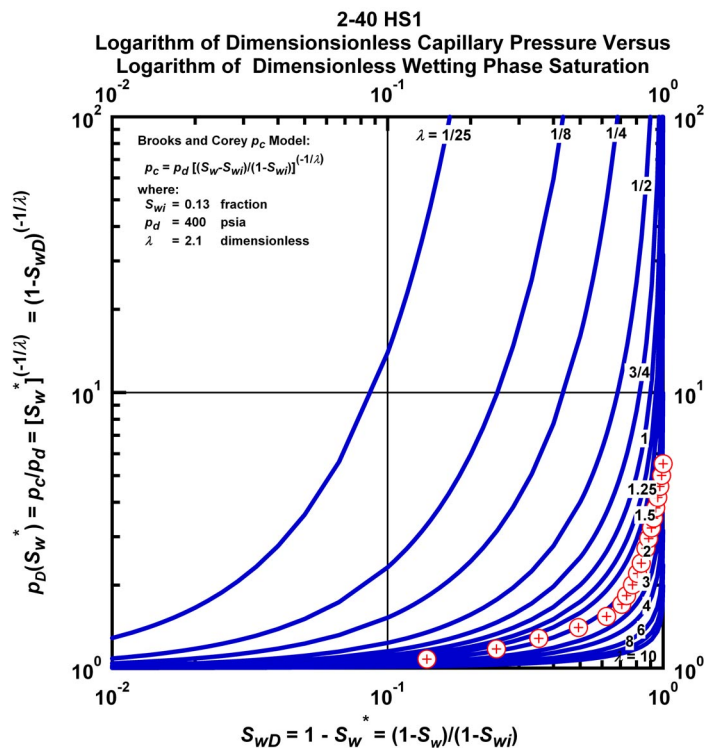


Figure 3.4 – Dimensionless capillary pressure versus dimensionless wetting phase saturation plot – Log-Log format "Type curve" for capillary pressure.

We believe that this "separate" calibration of the $p_c(S_w)$ data-model is appropriate, and we note that the majority of the effort in our correlation work focused on this particular task.

Estimation of k , p_d and λ Using Regression

The regression setup for Eqs. 3.8-3.10 is fairly straightforward, as we used the Solver Module in Microsoft Excel⁶⁴ to perform our regression work. We formulated each regression problem in terms of the sum-of-squared residuals (SSQ), sum-of-absolute relative error (ARE) and — depending on the case — these regressions were performed using the residual or absolute relative error based on the logarithm of a particular variable. A summary of our results for the k , p_d and λ regressions is given in **Table 3.1**.

Table 3.1 – Summary Regression Statistics for k , p_d , λ — Power Law Models

Case	Fig.	SSQ^* (ln(unit) ²)	ARE (percent)
k	2	2.3865 ln(md) ²	26.4580
p_d	3	1.2239 ln(psia) ²	22.2482
λ	4	1.0262	18.9111

* SSQ statistics based on $\ln(k)$, $\ln(p_d)$, and λ , respectively.

We present the results of our permeability (k) optimization in **Fig. 3.2**. We note excellent agreement between the measured permeabilities and those calculated from Eq. 3.8. The optimized coefficients from the regression analysis of Eq. 3.8 are summarized in **Table 3.2**.

Table 3.2 – Regression Summary for k

Optimized coefficients for k (Eq. 3.8):

Coefficient	Optimized Value
a_1	1233562.51 md
a_2	-1.8139352
a_3	1.4385928
a_4	2.2764176
a_5	1.7296397

Statistical summary for k (Eq. 3.8):

Statistical Variable	Value
Sum of Squared Residuals	2.3865 ln(md) ²
Variance	369278.5839 md ²
Standard Deviation	607.6830 md
Average Absolute Error	26.4580 percent

Substituting the coefficients from **Table 3.2** into Eq. 3.8, we have:

$$k = 1233562.52 \frac{1}{(p_d)^{1.8139}} \left[\frac{\lambda}{\lambda + 2} \right]^{1.4385} (1 - S_{wi})^{2.2764} \phi^{1.7296} \dots\dots\dots (3.11)$$

We note that Eq. 3.11 was used to calculate the entire permeability range — from low permeability (tight gas sands) to unconsolidated sands. From our perspective, the generalized permeability relation (Eq. 3.8) has theoretical rigor (see Appendix A) and may be a "universal" permeability model — valid for different lithologies, pore systems, and pore structures.

We recommend that the generalized form (Eq. 3.8) continue to be tested systematically. We will (again) note that care must be taken in assessing $p_c(S_w)$ suitable for such correlations. We have elected to consider Hg-air systems only for simplicity — extensions to other systems must continue systematically, with diligent data screening and a "simplest" model first mentality. In addition to our "power law" correlation, we also developed a number of different parametric models (Appendix E), as well as a non-parametric regression (Appendix H). These additional regressions provide insight into viability of correlations for the k variables. The most complex models most likely "over-fit" the data for a given correlation.

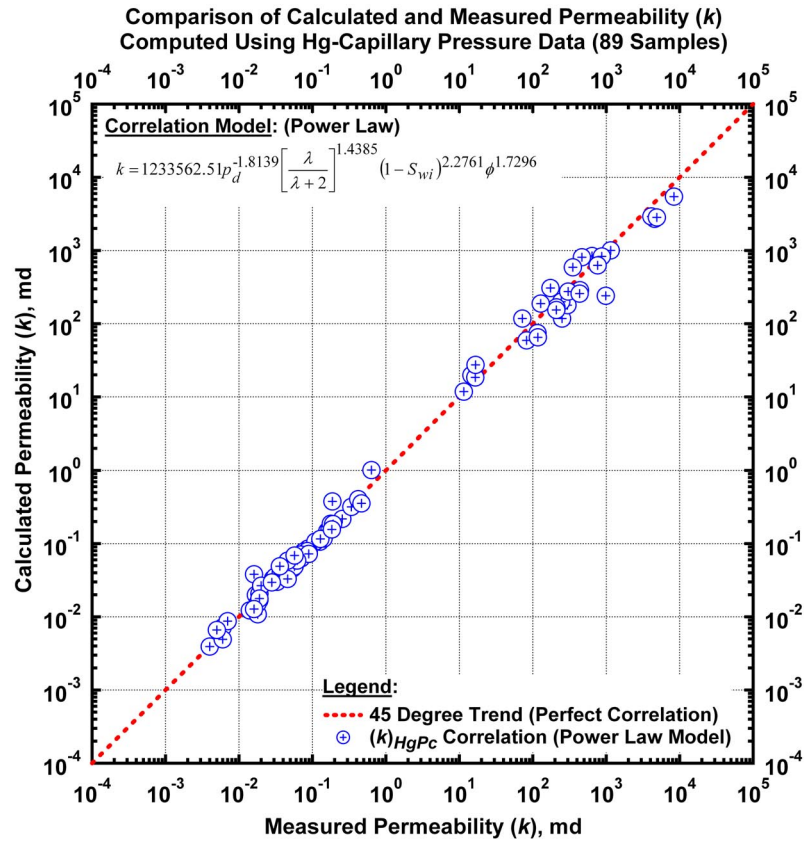


Figure 3.5 – Permeability correlation based on mercury capillary pressure data (Eq. 3.8 used for regression).

We also correlate the capillary displacement pressure with permeability, porosity and irreducible wetting phase saturation — the results of which are shown in **Fig. 3.5** using a power law correlation model (the regression summary for this case is given in **Table 3.3**). Although we have developed more complex models for the correlating the displacement pressure (Appendix F), we believe that Eq. 3.12 is an excellent "general" model. We also note that Thomas, Katz, and Tek⁶⁵ proposed a similar formulation, where this model is also plotted on **Fig. 3.5** for comparison.

Table 3.3– Regression Summary for p_d (Eq. 3.9)

Optimized coefficients for p_d (Eq. 3.9):

Coefficient	Optimized Value
b_1	751.3360 (psia)
b_2	0.8469
b_3	-0.5166
b_4	0.0489

Table 3.3 – continued

Statistical summary for p_d (Eq. 3.9):

Statistical Variable	Value
Sum of Squared Residuals	1.2239 ln(psia) ²
Variance	113392.3297 psia ²
Standard Deviation	336.7378 psia
Average Absolute Error	22.2482 percent

Substituting the coefficients in **Table 3.3** into Eq. 3.9, we have:

$$p_d = 751.3360 \phi^{0.8469} k^{-0.5166} (1 - S_{wi})^{0.0489} \dots\dots\dots (3.12)$$

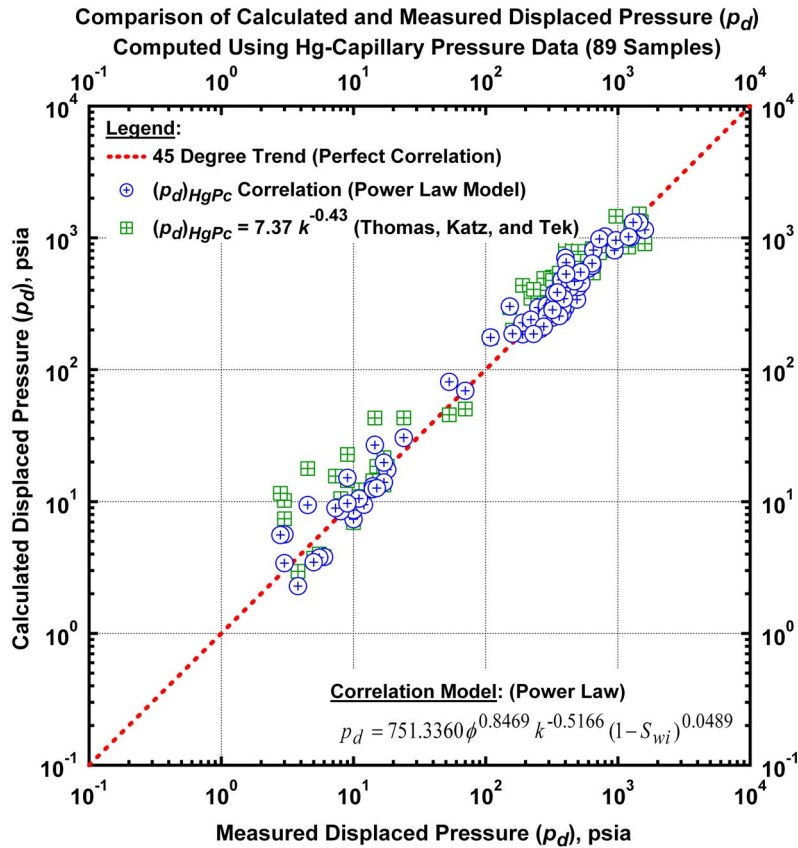


Figure 3.6 – Displacement pressure (p_d) correlation based on mercury capillary pressure data (Eq. 3.9 used for regression).

In our effort to correlate the index of pore-size distribution (λ) with permeability, porosity, irreducible wetting phase saturation and displacement pressure, we found less conformity in the resultant correlations. We believe that this behavior is due to the character of the index of pore-size distribution — recall that this parameter is an exponent in the Brooks-Corey $p_c(S_w)$ relation (Eq. 3.3). We have observed that Eq. 3.3 is relatively unaffected by the λ -parameter (*i.e., the model is relatively insensitive to the λ -parameter*).

In addition, we believe this insensitivity may make it more difficult to estimate the λ -parameter initially from $p_c(S_w)$ data than correlating the λ -parameter against other variables. Regardless, our characterization and correlation of the λ -parameter was less successful than our correlation of permeability (k) and capillary displacement pressure (p_d).

We present the correlation of the λ -parameter using a power law model in **Fig. 3.6**, and we present the regression summary for this case in **Table 3.4**.

Table 3.4– Regression Summary for λ (Eq. 3.10)

Optimized coefficients for λ (Eq. 3.10):

Coefficient	Optimized Value
c_1	0.00084
c_2	-1.0485
c_3	0.5498
c_4	-2.2790
c_5	0.9939

Statistical summary for λ (Eq. 3.10):

Statistical Variable	Value
Sum of Squared Residuals	1.0262
Variance	0.1943
Standard Deviation	0.4408
Average Absolute Error	18.9111 percent

Substituting the coefficients in **Table 3.4** into Eq. 3.10, we have:

$$\lambda = 0.00084 \phi^{-1.0485} k^{0.5498} (1 - S_{wi})^{-2.2790} p_d^{0.9939} \dots\dots\dots (3.13)$$

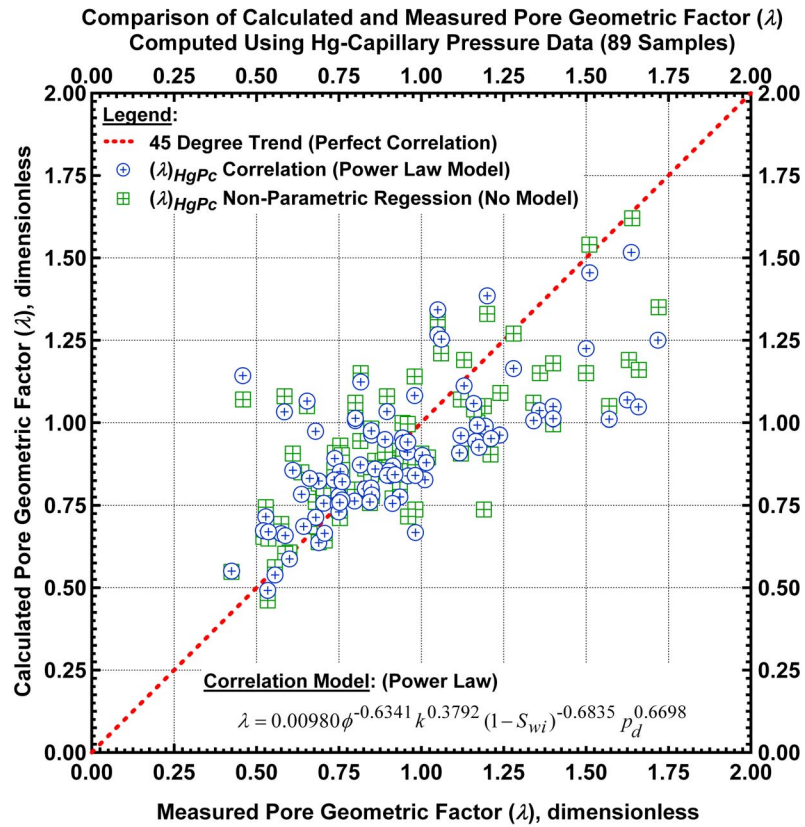


Figure 3.7 – Pore geometric factor (λ) correlation based on mercury capillary pressure data.

Our correlation of the λ -parameter yielded the weakest results (in terms of a graphical comparison (**Fig. 3.7**), not in terms of a statistical regression). The results shown in **Fig. 3.7** clearly show relatively weak conformance of the model to the data (*i.e.*, the blue circle symbols, relative to the red dashed line (perfect correlation)). To better understand (but probably not quantify) this deviation, we have also constructed a "non-parametric" correlation of the λ -parameter (Appendix G) using the methods given in ref. 66.

*A non-parametric correlation is the optimal statistical relationship for a given data set on a point-by-point basis — any parametric (*i.e.*, functional) correlation which yields better statistical metrics than the corresponding non-parametric correlation has "over-fitted" the data (*i.e.*, fitted the errors in the data).*

Our non-parametric correlation of the λ -parameter for this case is shown by the green square symbols on **Fig. 3.7**. The relative similarity of the data in **Fig. 3.7** suggest that our non-parametric correlation and our correlation using a power law model are comparable — which validates our use of the (relatively simple) power law model for this case.

As closure for this discussion regarding the correlation of the λ -parameter, we believe that the very basis of the λ -parameter (it is an exponent), coupled with the quality of data used to define the λ -parameter are the causes of the relatively weak correlation of the λ -parameter shown in **Fig. 3.7**. Based on the non-parametric correlation for this case, we do not recommend additional efforts to improve the parametric correlation. But, we do suggest recasting the problem so that permeability is directly related to the various measurable rock properties, including porosity (ϕ), irreducible wetting phase saturation (S_{wi}), and displacement pressure (p_d). We also recommend use of some parameter other than the index of pore-size distribution (λ) to represent the "curvature" of the capillary pressure curve. Finally, we would also comment that Eq. 3.13 (*i.e.*, the power law correlation for the λ -parameter) is probably more than sufficient for practical applications.

CHAPTER IV

SUMMARY, CONCLUSIONS, AND RECOMMENDATIONS FOR FUTURE WORK

4.1 Summary

Using the relations of Purcell,¹ Burdine,² Brooks and Corey,⁴ Wyllie and Spangler,³ and Nakornthap and Evans⁶³ we have developed a base model to correlate permeability from mercury capillary pressure data — our *base model* for permeability is given as:

$$k = 10.66 \frac{\omega}{n} (\sigma_{Hg-air} \cos \theta)^2 (1 - S_{wi})^3 \phi^3 \frac{1}{p_d^2} \left[\frac{\lambda}{\lambda + 2} \right] \dots\dots\dots (4.1)$$

Generalizing Eq. 4.1 into a correlation form yields:

$$k = a_1 \frac{1}{(p_d)^{a_2}} \left[\frac{\lambda}{\lambda + 2} \right]^{a_3} (1 - S_{wi})^{a_4} \phi^{a_5} \dots\dots\dots (4.2)$$

Eq. 4.2 suggests (under the assumptions of a "bundle of capillary tubes," Darcy's law, and other constraints which are related to how the capillaries are connected) that we can consider permeability to be a *power law* function of ϕ , S_{wi} , p_d , and λ . We recognize this simplicity, but we also suggest that Eq. 4.1 (or Eq. 4.2) are good starting points for the correlation of permeability. We used a reasonably large database of 89 samples (Hg capillary pressure data), to construct our correlations. This database includes k and ϕ data — as well as the S_{wi} , p_d , and λ -parameters obtained via analysis of the Hg capillary pressure data using the Brooks-Corey capillary pressure equation, given below:

$$p_c = p_d \left[\frac{S_w - S_{wi}}{1 - S_{wi}} \right]^{-\frac{1}{\lambda}} \dots\dots\dots (4.3)$$

Summarizing our work to date, we achieved the following power law correlations:

$k = f(\phi, S_{wi}, p_d, \lambda)$: **Fig. 3.5**

$$k = 1017003.2395 \frac{1}{(p_d)^{1.7846}} \left[\frac{\lambda}{\lambda + 2} \right]^{1.6575} (1 - S_{wi})^{0.5475} \phi^{1.6498} \dots\dots\dots (4.4)$$

$p_d = f(\phi, k, S_{wi})$: **Fig. 3.6**

$$p_d = 640.0538 \phi^{0.8210} k^{-0.5285} (1 - S_{wi})^{0.8486} \dots\dots\dots (4.5)$$

$\lambda = f(\phi, k, S_{wi}, p_d)$: **Fig. 3.7**

$$\lambda = 0.00980 \phi^{-0.6341} k^{0.3792} (1 - S_{wi})^{-0.6835} p_d^{0.6698} \dots\dots\dots (4.6)$$

The results of our modeling efforts suggest that the correlating properties of the porous media (k , ϕ , S_{wi} , p_d , and λ) are not specifically dependent upon lithology — but rather, these properties uniquely quantify the fluid flow behavior of the porous medium. In that sense, we see this work as a generalized correlation for flow in porous materials — including soils, filters, sintered metals, bead packs, and porous rocks. As we noted earlier, we believe that this work is applicable to carbonates with an inter-granular type of porosity — not to cases of "vuggy" carbonates.

We used the simple power law models to validate the "Timur" permeability relation (ref. 42) used since the late 1960's to estimate permeability from well logs (see Appendix C for proof). The basis for the Timur relation is empirical, but our work provides insight into the viability of the Timur relation as a generic model for permeability.

In addition to our "power law" correlations, we also developed a number of different parametric models (permeability — Appendix E, displacement pressure — Appendix F, pore geometric factor — Appendix G), as well as a non-parametric regression for each parameter. These additional regressions provide insight into viability of correlations for the k , p_d , and λ variables. We are satisfied that we have developed appropriate correlations for each variable, but also acknowledge that the most complex models most likely "over-fit" the data for a given correlation. Regardless, we put forth these models for further validation and utilization by the petrophysics discipline.

4.2. Conclusions

The following conclusions have been derived from this work:

1. The permeability (k) can be successfully correlated to the porosity (ϕ), capillary displacement pressure (p_d), irreducible wetting-phase saturation (S_{wi}), and the index of pore-size distribution (λ) using a theoretically defined power law correlation model (as well as other, more complex models).
2. The capillary displacement pressure (p_d) can also be correlated using a power law model to the permeability (k), porosity (ϕ), and irreducible wetting-phase saturation (S_{wi}). This observation confirms the fundamental work proposed Thomas, Katz, and Tek⁶⁵. Additional (and more complex) correlations confirm the inter-relation of the displacement pressure with permeability, porosity, and irreducible wetting-phase saturation.

3. The correlation of the index of pore geometry index (λ) is somewhat problematic — the λ -parameter may be only weakly defined by the k , ϕ , S_{wi} , and p_d variables. We find that the proposed λ -models are relatively weak — this is an issue that is most likely related to the quality and character of the capillary pressure data.

4.3 Recommendations for Future Work

The following recommendations are proposed:

1. Consideration of more complex correlation models for:

$$k = f(\phi, S_{wi}, p_d, \lambda)$$

$$p_d = f(\phi, k, S_{wi})$$

$$\lambda = f(\phi, k, S_{wi}, p_d)$$

Our experience with non-parametric regression⁶⁶ as applied to this work suggests that the proposed power law models are sufficient, and we would warn against "over-fitting" data in this work with excessively complex data models.

2. Extension of the results of this work to liquid-liquid and gas-liquid systems.

NOMENCLATURE

Field Variables (*Formation and Fluid Parameters*)

D_d	=	dominant grain size from petrological observation, mm
D_g	=	geometric mean diameter, mm
k	=	permeability, md or cm^2
L_i	=	effective length of flow path, cm
L_{tot}	=	actual length of flow path, cm
p_d	=	displacement pressure, psi
p_c	=	capillary pressure, psi
R_{35}	=	pore throat radius at an Hg saturation of 35 percent, μm
r_{eff}	=	effective pore radius, cm
R_i	=	incremental pore entry radius, cm
\bar{R}_i	=	average pore entry radius, cm
R_o	=	resistivity of formation at $S_w=1.0$, ohm-m
R_w	=	resistivity of formation brine, ohm-m
S_b	=	Hg saturation, fraction of <i>bulk</i> volume
$S_{b\infty}$	=	Hg saturation at $p_c = \infty$, fraction of <i>bulk</i> volume
S_{wi}	=	irreducible saturation, fraction
S_w	=	water saturation in the actual porous medium, fraction
S_w^*	=	water saturation in the model porous medium, fraction
V_i	=	incremental pore volume filled by mercury, cm^3
X_i	=	tortuosity factor ($X_i=L_i/L_{tot}$), fraction
γ	=	interfacial tension, dynes/cm
ϕ	=	porosity, fraction of pore volume
θ	=	contact angle, degrees
σ	=	interfacial tension, dynes/cm
$\sigma_{\text{Hg-air}}$	=	mercury-air interfacial tension, dynes/cm
θ	=	contact angle of incidence for wetting phase, radians

Dimensionless Variables

a	=	empirical constant defined by Archie
F_p	=	Purcell lithology factor, dimensionless
F_g	=	Thomeer pore geometrical factor, dimensionless
F_{WS}	=	Wyllie-Spangler shape factor, dimensionless
$J(S_w)$	=	dimensionless capillary pressure-saturation function
$J(S_w)_{1.0}$	=	dimensionless capillary pressure function at $S_w = 1.0$
m	=	cementation factor defined by Archie dimensionless (~ 2)
β	=	geometrical factor in the model porous medium
λ	=	index of pore-size distribution or pore geometric factor
η	=	number of pore throats/pore body as defined by Nakornthap and Evans dimensionless
ω	=	pore throat "impedance" factor, dimensionless
τ	=	tortuosity index

REFERENCES

1. Purcell, W.R.: "Capillary Pressures-Their Measurement Using Mercury and the Calculation of Permeability", *Trans. AIME*, (1949), **186**, 39
2. Burdine, N. T.: "Relative Permeability Calculations from Pore Size Distribution Data", *Trans. AIME*, (1953), **198**, 71.
3. Wyllie, M.R.J., and Gardner, G.H.F.: "The Generalized Kozeny–Carman Equation: Part II," *World Oil*, (1958), **146**(5): 210–228.
4. Brooks, R. H., and Corey, A. T.: "Properties of Porous Media Affecting Fluid Flow," *Journal Irrigation and Drainage Division ASCE*. (1966) **92**: 61-88.
5. Li, K. and Horne, R.N.: "Experimental Verification of Methods to Calculate Relative Permeability Using Capillary Pressure Data," paper SPE 76757 presented at the 2002 SPE Western Regional/ AAGP Pacific Section Joint Meeting held in Anchorage, AL, 20 – 22 May.
6. Ali, L., personal communication with T. Blasingame, Dept of Petroleum Engineering, Texas A&M University (1995)
7. Archie, G.E.: "The Electrical Resistivity Log as an Aid in Determining Some Reservoir Characteristics," *JPT* (1942), **5**:1-8
8. Neasham, J.W.: "The Morphology of Dispersed Clay in Sandstones Reservoirs and Its Effect on Sandstones Shaliness, Pore Space and Fluid Flow Properties," paper SPE 6858 presented at the 1977 Annual Technical Conference and Exhibition held in Denver, CO, October 9-12.
9. Amyx, J.W., Bass, D.M. and Whiting, R.L.: *Rock Properties: Petroleum Reservoir Engineering* in McGraw-Hill Book Co. Inc., New York (1960).
10. McCullough, F.W., Thornton, O.F. and Bruce, W.A.: "Determination of the Interstitial-Water Content of Oil and Gas Sand by Laboratory Tests of Core Samples," *Drill. & Prod Prac. API* (1944), 180-188.
11. Thornton, O.F. and Marshall, D.L.: "Estimating Interstitial Water by the Capillary Pressure Method," *Trans. AIME*, (1947) **170**, 69-80.
12. Bruce, W.A. and Welge, H.J.: "Restored-State Method for Determination of Oil-in-Place and Connate Water," *Oil & Gas J.*, (1947), **46**, 22-23.
13. Rose, W. and Bruce, W.A.: "Evaluation of Capillary Character in Petroleum Reservoir Rock," *Trans. AIME*, (1949) **186**, 127-142.
14. Hassler, G.L., and Brunner, E.: "Measurements of Capillary Pressure in Small Core Samples," *Trans. AIME*, **160**, 114-123.
15. Slobod, R.L., Chambers, A., and Prehn, W.L.: "Use of Centrifuge for Determining Connate Water, Residual Oil, and Capillary Pressure Curves of Small Core Samples," *Trans. AIME*, (1951), **192**, 127-134,
16. Hoffman, R.N.: "A Technique for the Determination of Capillary Pressure Curves Using a Constantly Accelerated Centrifuge". *Trans AIME*, (1963) **228**, 227-235.
17. Christiansen, R.L.: "Geometric Concerns for Accurate Measurement of Capillary Pressure Relationships with Centrifuge Methods," *SPE Formation Evaluation*, (1992) **7**, 311-314.
18. Forbes P.L., Chen Z. and Ruth D.: "Quantitative Analysis of Radial Effects on Centrifuge Capillary Pressure Curves", paper 28182 presented at the 1995 SPE Annual Technical Conference and Exhibition, New Orleans, September 26-29.

19. O'Meara, D.J., Hirasaki, G.J. and Rohan, J.A.: "Centrifuge Measurements of Capillary Pressure: Part 1-Outflow Boundary Condition," paper SPE 18296 presented at the 1988 SPE Annual Technical Conference and Exhibition, Houston, TX, October 2-5.
20. Hirasaki, G.J., O'Meara, D.J. and Rohan, J.A.: "Centrifuge Measurements of Capillary Pressure: Part 1-Cavitation," paper SPE 18592 presented at the 1988 SPE Annual Technical Conference and Exhibition, Houston, TX, October 2-5.
21. Chen, Z.A. and Ruth, D.W.: "Centrifuge Capillary Pressure Data Interpretation: Gravity Degradation Aspect Consideration," SCA paper 9425 presented at the 1994 Society of Core Analysts Annual Conference, Stavanger, Norway, September 12-14.
22. Melrose, J.C., Dixon, J.R., and Mallinson, J.E.: "Comparison of Different Techniques for Obtaining Capillary Pressure Data in Low-Saturation Region," paper SPE 22690 presented at the 1994 SPE Annual Technical Conference & Exhibition, Dallas, TX, October 6-9.
23. Morrow, N.R., Brower, K.R., and Kilmer, N.H.: "Relationships of Pore Structure to Fluid Behavior in Low Permeability Gas Sands", Final Report, DOE/BC/10216-13 (DE84012721), U.S. Dept. of Energy, Bartlesville (Sept., 1984), 60-71.
24. Corey, A. T.: "The Interrelation between Gas and Oil Relative Permeabilities," *Prod. Mon.*, (1954), **19**, 38.
25. Thomeer, J. H.: "Introduction of a Pore Geometrical Factor Defined by the Capillary Pressure Curve," *JPT* (1960), 73-77.
26. van Genuchten, M. Th.: "A Closed-Form Equation for Predicting the Hydraulic Conductivity of Unsaturated Soils," *Soil Sci. Soc. Am. J.* (1980), **44**, 892-898.
27. Jing, X.D. and Van Wunnik, J.N.M.: "A Capillary Pressure Function for Interpretation of Core-Scale Displacement Experiments," SCA 9807, Proceedings of 1998 International Symposium of the Society of Core Analysts, The Hague, Netherlands, Sept. 14-16, 1998.
28. Li, K. and Horne, R.N.: "Experimental Verification of Methods to Calculate Relative Permeability Using Capillary Pressure Data," Paper SPE 76757 presented at the 2002 SPE Western Regional/ AAGP Pacific Section Joint Meeting held in Anchorage, AK, May 20 - 22.
29. Skelt, C.H. and Harrison, B.: "An Integrated Approach to Saturation Height Analysis," Paper NNN, Proceedings of 36th SPWLA Annual Symposium, June 26-29, 1995.
30. Lenormand, R.: "Gravity-Assisted Inert Gas Injection: Micromodel Experiments and Model Based on Fractal Roughness," paper presented at the 1990 European Oil and Gas Conference, Altavilla Milica, Palermo, Sicily, October 9-12.
31. Archie, G.E.: "The Electrical Resistivity Log as an Aid in Determining Some Reservoir characteristics," *JPT* (1942), **5**, 1-8
32. Jennings, J. and Lucia, F.J.: "Predicting Permeability from Well Logs in Carbonates with a Link to Geology for Interwell Permeability Mapping," Paper 71336, presented at the 2001 SPE Annual Technical Conference and Exhibition held in New Orleans, LA, 30 September-3 October.
33. Cazier, E.C. Hayward, A.B. Espinosa, G.. Velandia, J Mugniot, J-F. and Leel, Jr., W.G.: "Petroleum Geology of the Cusiana Field, Llanos Basin Foothills, Colombia," *AAPG Bulletin*, (October 1995), **79**, 1444-1463.
34. Berg, R.R.: "Method for Determining Permeability from Reservoir Rock Properties," *Transactions — Gulf Coast Association of Geological Societies* (1970), **XX**, 303-335.
35. Kozeny, J.: "Uber-Kapillare Leitung des Wassers in Boden, Sitzungsberichte," *Wasserkraft und Wasserwirtschaft* (1927) **22**, 67-86.
36. Carman, P.C.: "Fluid Flow through Granular Beds," *Trans.*, AICE (1937) **15**, 150-166.

37. Krumhein. W.. and C;. Monk.: "Permeability as a Function of the Size Parameters of Unconsolidated Sand," *Trans. AIME*, (1944) **151**, 153-163.
38. Beard, D., and Weyl, P.: "Influences of Texture on Porosity of Unconsolidated Sand," *AAPG Bulletin*, (1973) **57**, 349-369
39. Nelson P.H.: "Permeability—Porosity Relationships in Sedimentary Rocks," *Log Analyst* (1984), **3**, 38—62.
40. van Baaren, J.: "Quick Look Permeability Estimates Using Sidewall Samples and Porosity Logs," SPWLA Sixth European Symposium Transaction, March 1979.
41. Wyllie M.R. and Spangler M. B.: "The Application of Electrical Resistivity Measurements to the Problem of Fluid Flow in Porous Media," *Research Project 4-G-1 Geology Division Report No. 15* (March 1951) Gulf Research and Development Company.
42. Timur, A.: "An Investigation of Permeability, Porosity, and Residual Water Saturation Relationships for Sandstone Reservoirs," *The Log Analyst* (1968), **9**, 30-48.
43. Coates, G.R. Peveraro, R.C.A., Hardwick, A. and Roberts, D.: "The Magnetic Resonance Imaging Log Characterized by Comparison With Petrophysical Properties and Laboratory Core Data," paper SPE 22723, presented at the 1991 Annual Technical Conference and Exhibition of the Society of Petroleum Engineers held in Dallas, TX, October 6-9.
44. Rodriguez, A.: "Facies Modeling and the Flow Unit Concept as a Sedimentological Tool in Reservoir Description: A Case Study," Paper SPE 18154, presented at the 1988 Annual Technical Conference and Exhibition of the Society of Petroleum Engineers held in Houston, TX, October 2-5
45. Quintero, L., Boyd, A. Gyllensten, A., and El Wazeer, F.: "Comparison of Permeability from NMR and Production Analysis in Carbonate Reservoirs," paper SPE 56798 presented at the 1999 Annual Technical Conference and Exhibition of the Society of Petroleum Engineers held in Houston, TX, October 3-6.
46. Katz, A.J. and Thompson, A.H.: "Quantitative Prediction of Permeability in Porous Rock," *Phys. Rev. B* (December 1986) **34**, No. 11, 8179.
47. Mavko, G. and Nur, A.: "The Effect of a Percolation Threshold in the Kozeny-Carman Relation," *Geophysics* (September–October 1997) **62**, No. 5, 1480.
48. Martys, N.S., Torquato, S., and Bentz, D.P.: "Universal Scaling of Fluid Permeability for Sphere Packings," *Phys. Rev. E* (July 1994) **50**, No. 1, 403.
49. Pape, H., Clauser, C., and Joachim, I.: "Permeability Prediction Based on Fractal Pore-Space Geometry," *Geophysics* (September–October 1999) **64**, No. 5, 1447.
50. Muller, J. and McCauley, J.L.: "Implication of Fractal Geometry for Fluid Flow Properties of Sedimentary Rocks," *Trans. in Porous Med.* (June 1992) **8**, No. 2, 133.
51. Wong, P.: "The Sedimentary Physics of Sedimentary Rock," *Physics Today* (December 1988) 24.
52. Hansen, J.P. and Skjeltorp, A.T.: "Fractal Pore Space and Rock Permeability Implications," *Phys. Rev. B* (1 August 1988) **38**, No. 4, 2635.
53. Garrison, J.R., Pearn, W.C., and von Rosenberg, D.U.: "The Fractal Menger Sponge and Sierpinski Carpet," *In-situ* (1992) **17**, 1-54
54. Leverett, M.C.: "Capillary Behavior in Porous Solids," *Trans, AIME* **142** (1941), 341-358.
55. Calhoun, J.C., Lewis, M. and Newman, R.C.: "Experiments on the Capillary Properties of Porous Solids," *Trans., AIME* (1949) **186**, 189-196.
56. Burdine, N.T., Gournay, L.S., and Reichertz, P.P.: "Pore Size Distribution of Petroleum Reservoir Rocks", *Trans. AIME*, (1950), **189**, 195-204.

57. Thomeer, J.H.M.: "Air Permeability as a Function of Three Pore-Network Parameters," *JPT* (April 1983), 809-814.
58. Swanson, B.F.: "A Simple Correlation between Permeabilities and Mercury Capillary Pressures," *JPT*, (Dec. 1981), 2488-2504.
59. Wells, J.D. and Amaefule, J.O.: "Capillary Pressure and Permeability Relationships in Tight Gas Sands," paper SPE 13879 presented at the 1985 Low Permeability Gas Reservoir held in Denver, CO, May 19-22.
60. Kolodzie, S., Jr.: "Analysis of Pore Throat Size and Use of the Waxman-Smits Equation to Determine *OOIP* in Spindle Field, Colorado," paper SPE 9382 presented at the 1980 Annual Fall Technical Conference of Society of Petroleum Engineers held in Dallas, TX, Sept. 21-24.
61. Pittman, E.D.: "Relationship of Porosity and Permeability to Various Parameters Derived from Mercury Injection-Capillary Pressure Curves for Sandstone," *AAPG Bull.* (1992), **76**, No. 2 191-198.
62. Klinkenberg, L.J.: "The Permeability of Porous Media to Liquids and Gases," paper presented at the API 11th Mid-Year Meeting, Tulsa, OK (May 1941); in *API Drilling and Production Practice* (1941) 200-213.
63. Nakornthap, K. and Evans, R.D.: "Temperature-Dependent Relative Permeability and Its Effect on Oil Displacement by Thermal Methods," *SPE* (May 1986) 230-242.
64. Microsoft® Office *Excel* 2003, Microsoft Corporation (1985-2003).
65. Thomas, L.K., Katz, D.L., and Tek, M.R.: "Threshold Pressure Phenomena in Porous Media," *SPEJ* (June 1968) 174-183.
66. Breinan, L. and Friedman, J.: "Estimation Optimal Transformations for Multiple Regression and Correlation," *Journal of the American Statistical Association* (1985), **80**, No. 391, 122-144.

APPENDICES

The following appendices are in separate files.

- APPENDIX A DERIVATION OF PERMEABILITY AND RELATIVE PERMEABILITY FROM CAPILLARY PRESSURE
- APPENDIX B DERIVATION OF A FUNCTION FOR THE NORMALIZATION OF CAPILLARY PRESSURE CURVES.
- APPENDIX C COMPARISON WITH TIMUR'S PERMEABILITY MODEL
- APPENDIX D SUMMARY OF DATA USED IN THIS STUDY
- APPENDIX E CORRELATIONS FOR PERMEABILITY (k) DERIVED FROM THE DATA IN THIS WORK
- APPENDIX F CORRELATIONS FOR DISPLACEMENT PRESSURE (p_d) DERIVED FROM THE DATA IN THIS WORK
- APPENDIX G CORRELATIONS FOR PORE GEOMETRIC FACTOR (λ) DERIVED FROM THE DATA IN THIS WORK
- APPENDIX H NON-PARAMETRIC REGRESSIONS DERIVED FROM THE DATA IN THIS WORK
- APPENDIX I LIBRARY OF CAPILLARY PRESSURE VERSUS WETTING PHASE SATURATION PLOTS —CARTESIAN CAPILLARY PRESSURE FORMAT
- APPENDIX J LIBRARY OF CAPILLARY PRESSURE VERSUS WETTING PHASE SATURATION PLOTS — LOGARITHMIC CAPILLARY PRESSURE FORMAT
- APPENDIX K LIBRARY OF CAPILLARY PRESSURE VERSUS NORMALIZED WETTING PHASE SATURATION PLOTS — LOGARITHMIC CAPILLARY PRESSURE FORMAT
- APPENDIX L LIBRARY OF DIMENSIONLESS CAPILLARY PRESSURE VERSUS NORMALIZED WETTING PHASE SATURATION PLOTS — LOG-LOG FORMAT "TYPE CURVE" FOR CAPILLARY PRESSURE (BROOKS AND COREY CAPILLARY PRESSURE MODEL)

APPENDIX M LIBRARY OF DIMENSIONLESS CAPILLARY PRESSURE VERSUS
DIMENSIONLESS WETTING PHASE SATURATION PLOTS — LOG-LOG
FORMAT "TYPE CURVE" FOR CAPILLARY PRESSURE (BROOKS AND
COREY CAPILLARY PRESSURE MODEL)

APPENDIX N SUPPLEMENTAL REFERENCES

VITA

Name: Caroline Cécile Huet

Born: 28 April 1980
Blois (41) France

Permanent Address: 35 bis, rue Fortineau
41500 Mer
France
(carolinehuet@hotmail.com)

Education: Ecole Nationale Supérieure de Géologie, Nancy, France
Diplôme d'ingénieur
September 2003

Institut National Polytechnique de Lorraine, Nancy, France
DEA Terre, Dynamique, Ressources
September 2003

IFP School, Reuil-Malmaison, France
Master of Science Degree in Reservoir and Geoscience Engineering
May 2005

Texas A&M University, College Station, Texas, USA
Master of Science Degree in Petroleum Engineering
December 2005